PROCEEDINGS A

rspa.royalsocietypublishing.org

Research

Article submitted to journal

Subject Areas:
35Q86, 60F05, 86A15.

Keywords:
random medium, surface wave, body wave, mode coupling, radiative transfer, equipartition.

Author for correspondence:
J. Garnier
e-mail:
josselin.garnier@polytechnique.edu

THE ROYAL SOCIETY
PUBLISHING

Onset of energy equipartition among surface and body waves

L. Borcea[1], J. Garnier[2] and K. Sølna[3]

[1]Department of Mathematics, University of Michigan, Ann Arbor, MI 48109.
[2]CMAP, CNRS, Ecole polytechnique, Institut Polytechnique de Paris, 91128 Palaiseau Cedex, France; INRIA, France.
[3]Department of Mathematics, University of California at Irvine, Irvine, CA 92697.

We derive a radiative transfer equation that accounts for coupling from surface waves to body waves and the other way around. The model is the acoustic wave equation in a two-dimensional waveguide with reflecting boundary. The waveguide has a thin, weakly randomly heterogeneous layer near the top surface, and a thick homogeneous layer beneath it. There are two types of modes that propagate along the axis of the waveguide: those that are almost trapped in the thin layer, and thus model surface waves, and those that penetrate deep in the waveguide, and thus model body waves. The remaining modes are evanescent waves. We introduce a mathematical theory of mode coupling induced by scattering in the thin layer, and derive a radiative transfer equation which quantifies the mean mode power exchange. We study the solution of this equation in the asymptotic limit of infinite width of the waveguide. The main result is a quantification of the rate of convergence of the mean mode powers toward equipartition.

1. Introduction

The description of energy transfer between surface waves and body waves is of interest in seismology [20,29], ultrasonic inspection [32], manipulation of waves [8] and the development of surface acoustic wave devices like filters, resonators and scanners [28]. Radiative transfer [9] has been used for more than thirty years to describe wave propagation in heterogeneous media like the Earth's crust [20,25,31,34], biological tissue [3], the atmosphere and the ocean [2,16]. The mathematical theory of

radiative transfer in open space, which involves only body waves, is well established [4–6,13,24]. However, the coupling between surface waves propagating along boundaries and body waves remains a challenge [18,21,29,35] that is particularly relevant to understanding seismic coda, the long tail portion of seismograms. Because surface and body waves probe different parts of the Earth, methods like coda wave interferometry [23,30], passive image interferometry [26,27] and the extraction of Green's functions from cross-correlation of diffuse fields [7,14,17,19] rely on understanding the composition of the coda at increasing lapse time. It is expected that the power exchange between the surface and body waves evolves over time and eventually leads to equipartition [15,24,33]. But how does this evolution occur and on what time or propagation distance?

This question has motivated a number of recent studies: In [22] the sensitivity of coda waves to perturbations at different depths and for varying lapse time is studied via numerical simulations in a medium with random fluctuations of the pressure and shear wave velocity modeled by a von Kármán distribution with Hurst index 0.5. In [31] the authors study elastic wave mode coupling in a slab geometry using the Born scattering approximation. The Born approximation is also used in [18] to study elastic waves in a half space. A system of coupled integral equations that model the power exchange between surface and body waves is introduced in [35] using a phenomenological approach. The study in [21] considers acoustic waves in a heterogeneous medium with point scatterers, occupying the half-space. The authors impose an impedance (Robin) boundary condition, which leads to a unique wave mode trapped near the surface, whose penetration depth depends on the impedance condition. This model seeks to mimic the situation in seismology while minimizing the mathematical complexity. Using a phenomenological approach, based on the independent scattering approximation, the analysis in [21] predicts the equipartition of energy between surface and body waves at long lapse times. The mathematical analysis in [11] also uses the acoustic wave equation in the half space, but with a thin randomly inhomogeneous layer at the surface instead of an impedance boundary condition. This thin layer supports guided modes that play the role of surface waves, provided the index of refraction in the thin layer is larger than the one below it. This model makes it possible to describe the power transfer from the surface waves to the radiating modes, which play the role of body waves. However, the reverse power transfer is negligible [11].

In this paper we propose a two-dimensional waveguide model for studying the back and forth transfer of power between surface and body waves. The waveguide has two perfectly reflecting parallel boundaries at distance D, and contains a thin layer of width d, comparable to the wavelength and much smaller than D, adjacent to the top boundary and filled with a weakly randomly heterogeneous medium. The remaining part of the waveguide is filled with a homogeneous medium, as illustrated in Fig. 1. The advantage of the waveguide model is that it allows the decomposition of the wave field in a complete, countable set of modes that are either waves that propagate along the axis of the waveguide, or are evanescent waves. Among the propagating waves, a few are trapped within the thin random layer, and play the role of surface waves. The remaining propagating waves are body waves that are supported in the entire waveguide. The number and penetration depth of these surface waves depend on the thickness of the thin layer and the ratio between the indices of refraction in the thin layer and in the background homogeneous medium below it. Hence, this model mimics the situation in seismology with significant flexibility.

We use stochastic asymptotic analysis to analyze the coupling of the modes. The asymptotic parameter $\varepsilon \ll 1$ quantifies the small amplitude of the random fluctuations of the wave speed in the thin layer, and the waves propagate at large, ε-dependent distance, so that mode coupling induced by scattering becomes significant. The result of the asymptotic analysis in the limit $\varepsilon \to 0$ is a new radiative transfer equation that accounts for power exchange between all the modes. We study its solution in the regime $D \gg d$, so that we approach the half-space setting. We prove that

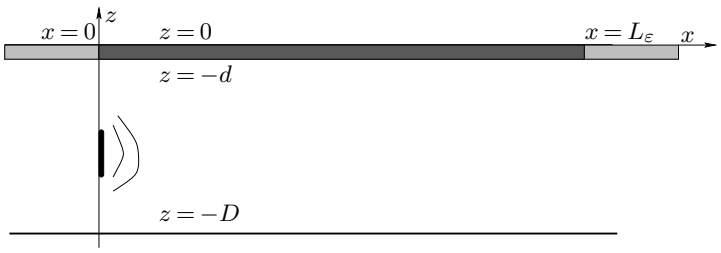

Figure 1. Illustration of the setup in a two-dimensional waveguide with reflecting boundaries at $z=0$ and $z=-D$. The direction of propagation of the waves is along the x (range) axis. The coordinate z is the cross-range. The random medium with average index of refraction $n>1$ lies in the subset $(0,L_\varepsilon)\times(-d,0)$, the thin layer shown with the darkest color. The medium in $\{\mathbb{R}\setminus(0,L_\varepsilon)\}\times(-d,0)$ is homogeneous with index of refraction n. The medium in $\mathbb{R}\times(-D,-d)$ is homogeneous with index of refraction 1. The source is supported at $x=0$, for z between $-D$ and 0.

an equipartition between surface and body waves is established at very large range [1] (propagation distance), but the dynamics is multiscale: at short range there is a quick evolution of the surface mode powers which leads to the establishment of a metastable distribution of power among these modes. This metastable distribution is uniform only under special circumstances, otherwise it depends on the effective coupling coefficients between the surface and body waves. At large range the body mode powers evolve slowly and they modify the metastable distribution of the surface mode powers, until the equilibrium equipartition is reached.

The main result can be summarized as follows: Let N be the number of propagating modes, which includes $N_{\rm s}\ll N$ surface wave modes and $N_{\rm b}=N-N_{\rm s}$ body wave modes, and let $P_j(x),\ j=1,\dots,N$, be their mean powers. The initial power distribution is determined by the source located at the origin of the range coordinate x, but mode coupling redistributes the power as x grows. We consider a smooth covariance function $\mathcal{C}$ of the random fluctuations of the index of refraction in the thin surface layer, and a scaling regime which gives weak backscattering. Therefore, the power redistribution can be described as an evolution problem i.e., the radiative transfer equation

$$\partial_x P_j(x)=\sum_{l=1}^{N}\Gamma^c_{jl}\big[P_l(x)-P_j(x)\big],\qquad x>0, \tag{1.1}$$

with constant $N\times N$ coupling matrix $\boldsymbol{\Gamma}^c=\big(\Gamma^c_{jl}\big)_{j,l=1}^N$. This matrix is defined in terms of the covariance $\mathcal{C}$ and the eigenvalues and eigenfunctions of the Sturm-Liouville (Helmholtz) operator $\partial_z^2+k^2{\rm n}_0^2(z)$ in the coordinate $z\in(-D,0)$, where ${\rm n}_0(z)$ is the index of refraction in the reference waveguide (without the random fluctuations). The eigenfunctions define the cross-range profiles of the modes.

Using the expression of $\boldsymbol{\Gamma}^c$, we identify and quantify three characteristic range scales on which the mean mode powers evolve:

1) The shorter scale, that gives the order of x where there is strong coupling among the surface modes, which drives their mean powers towards a metastable distribution.

2) The intermediate range scale, which defines the order of x where mode coupling results in a slow evolution of both the mean powers of the body modes and the metastable distribution of the mean powers of the surface modes.

3) The larger scale, which gives the order of x where the mean powers of the body modes evolve towards equipartition. As this occurs, the metastable equilibrium of the surface mode powers

[1] We study the wave propagation at fixed frequency and with large range, which corresponds to long lapse time in the time domain.

also becomes the uniform distribution, so the whole system arrives at a global equipartition with uniform mean mode power distribution.

The paper is organized as follows: We begin in section 2 with the setup. Then we describe in section 3 the propagating (surface and body wave) modes and the evanescent modes in the reference waveguide. These modes form a complete set used to expand the wave field in the randomly perturbed waveguide. The effective dynamics of the random mode amplitudes in the limit $\varepsilon \to 0$ is given in section 4. We also give there the radiative transfer equation for the mean mode powers. The main result of the paper, which is the characterization of the evolution of these powers and the convergence to equipartition in the regime with large D/d is in section 5. In section 6 we present numerical results for large D/d. We end with a summary in section 7.

2. Setup

We consider time-harmonic acoustic waves in a two-dimensional waveguide illustrated in Fig. 1. The waveguide is in the domain $(x, z) \in \mathbb{R} \times (-D, 0)$, where z is the depth (cross-range) coordinate and the range coordinate x is along the direction of propagation of the waves. The wave field $p(x, z)$ satisfies the Helmholtz equation,

$$\left[\partial_x^2 + \partial_z^2 + k^2 \mathrm{n}_\varepsilon^2(x, z)\right] p(x, z) = \delta'(x) f(z), \qquad (x, z) \in \mathbb{R} \times (-D, 0), \tag{2.1}$$

with boundary conditions

$$p(x, z = 0) = 0, \qquad \partial_z p(x, z = -D) = 0, \tag{2.2}$$

and radiation conditions at $|x| \to \infty$. Here k is the wavenumber calculated with the reference wave speed in the homogeneous medium occupying the bottom section $\mathbb{R} \times (-D, -d)$ of the waveguide. The thin layer $\mathbb{R} \times (-d, 0)$, with $0 < d < D$, is filled with a medium whose index of refraction has an average value that is larger than in the bottom section and is randomly fluctuating in the section $x \in (0, L^\varepsilon)$. We will take $D \gg d$ in section 5. The model of the index of refraction is

$$\mathrm{n}_\varepsilon^2(x, z) = \begin{cases} n^2 + \varepsilon \nu(x, z) & \text{if } (x, z) \in (0, L_\varepsilon) \times (-d, 0), \\ n^2 & \text{if } (x, z) \in \{\mathbb{R} \setminus (0, L_\varepsilon)\} \times (-d, 0), \\ 1 & \text{otherwise,} \end{cases} \tag{2.3}$$

with constant $n > 1$, so that there are nearly trapped modes in the thin layer, which play the role of surface waves. The fluctuations are modeled in (2.3) by the zero-mean, bounded, stationary in x random process $\nu(x, z)$, with covariance function

$$\mathcal{C}(x, z, z') = \mathbb{E}[\nu(x', z)\nu(x + x', z')]. \tag{2.4}$$

The typical amplitude of the fluctuations is small, as modeled by the small and positive dimensionless parameter ε. As a function of x, the covariance function is assumed to decay fast enough at infinity so that a diffusion-approximation theorem [10, Chapter 6] can be used. Specifically, $\mathcal{C}$ should belong to $L^{1/2}$ as a function of x. The dependence of $\mathcal{C}$ on x is also assumed to be smooth, or equivalently, its Fourier transform with respect to x is assumed to decay fast enough, so that the forward-scattering approximation that we discuss in section 4.(a) is valid. A typical example is the Gaussian covariance function (6.2).

The reference length scale is the wavelength $2\pi/k$, and the width d of the thin layer satisfies $kd = O(1)$, so that there is a finite number of surface waves. When $D \gg d$, the waveguide supports a large number of body waves, which is proportional to kD as explained below. We will see that the net scattering effect of the random fluctuations of the index of refraction becomes of order one at range distances of order ε^{-2}, so we consider the interesting case $L_\varepsilon = L/\varepsilon^2$. The fluctuations in (2.3) do not extend beyond the range L_ε, so we can set a radiation boundary condition at $x \to \infty$. We also assume that they are supported at positive range, because we focus attention on the propagation in the forward direction $x > 0$, away from the source modeled by the right-hand side

in equation (2.1). This source is localized at $x=0$ (it is proportional to the derivative of the Dirac $\delta(x)$) and has a transverse profile $f(z)$.

3. Waveguide modes

The stochastic analysis of the net scattering effect of the random medium uses the decomposition of the wave field in the orthonormal $L^2(-D,0)$ basis of the eigenfunctions $\big(\phi_j(z)\big)_{j\geq 1}$ of the Sturm-Liouville operator $\partial_z^2+k^2\mathrm{n}_0^2(z)$, with domain $\{\phi\in H^2(-D,0):\phi(0)=\partial_z\phi(-D)=0\}$ and coefficient

$$\mathrm{n}_0^2(z)=\begin{cases} n^2 & \text{if } z\in(-d,0),\\ 1 & \text{if } z\in(-D,-d).\end{cases} \tag{3.1}$$

This operator has a discrete spectrum $(\lambda_j)_{j\geq 1}$, with simple eigenvalues satisfying

$$\cdots<\lambda_j<\cdots<\lambda_1<n^2k^2, \qquad \lim_{j\to+\infty}\lambda_j=-\infty. \tag{3.2}$$

The waveguide modes are special solutions of the Helmholtz equation with index of refraction (3.1). They are waves with tranverse profile defined by the eigenfunctions, that propagate or decay along the x axis. Among the propagating modes, we distinguish those that are trapped in the thin layer, and thus model surface waves. The eigenfunctions that define them are described in section 3.(a). The other propagating modes penetrate in the whole cross-section of the waveguide, and thus model body waves. The eigenfunctions that define the body and the evanescent waves are described in section 3.(b). The mode wave decomposition in the reference (unperturbed) waveguide is in section 3.(c) and the decomposition in the random waveguide is in section 3.(d).

(a) The eigenfunctions that define the surface waves

Here we describe the eigenvalues $(\lambda_j)_{1\leq j\leq N_{\mathrm{s}}}$ in the spectral interval (k^2,n^2k^2), and the corresponding eigenfunctions

$$\phi_j(z)=\begin{cases} A_j\sin\big[z\sqrt{k^2n^2-\lambda_j}\big], & \text{if } z\in(-d,0),\\ B_j\cosh\big[(D+z)\sqrt{\lambda_j-k^2}\big], & \text{if } z\in(-D,-d).\end{cases} \tag{3.3}$$

The constants A_j and B_j are related by

$$B_j=-A_j\frac{\sin\big[d\sqrt{k^2n^2-\lambda_j}\big]}{\cosh\big[(D-d)\sqrt{\lambda_j-k^2}\big)\big]}, \tag{3.4}$$

so that $\phi_j(z)$ is continuous at $z=-d$, and A_j is defined, up to a sign, using the normalization $\int_{-D}^0\phi_j(z)^2dz=1$. The continuity of $\partial_z\phi_j(z)$ at $z=-d$ implies that the eigenvalue λ_j must be a solution of

$$-\tan\big[d\sqrt{k^2n^2-\lambda}\big]\tanh\big[(D-d)\sqrt{\lambda-k^2}\big]=\frac{\sqrt{k^2n^2-\lambda}}{\sqrt{\lambda-k^2}}. \tag{3.5}$$

When $kD\to+\infty$, we can approximate the eigenvalues by the solutions in (k^2,n^2k^2) of the simpler equation

$$-\tan\big[d\sqrt{k^2n^2-\lambda}\big]=\frac{\sqrt{k^2n^2-\lambda}}{\sqrt{\lambda-k^2}}. \tag{3.6}$$

As proved in appendix A, there are

$$N_{\mathrm{s}}=\left\lceil\frac{kd\sqrt{n^2-1}}{\pi}-\frac{1}{2}\right\rceil \tag{3.7}$$

such solutions, where the brackets denote the ceil part, meaning that N_s is the unique integer such that $(N_s - 1/2)\pi < kd\sqrt{n^2-1} \leq (N_s + 1/2)\pi$. We assume that $N_s \geq 1$, i.e. $kd\sqrt{n^2-1} > \pi/2$. The eigenfunctions have the form

$$\phi_j(z) = \begin{cases} A_j \sin\left[z\sqrt{k^2n^2-\lambda_j}\right], & \text{if } z \in (-d, 0), \\ -A_j \sin\left[d\sqrt{k^2n^2-\lambda_j}\right] \exp\left[(d+z)\sqrt{\lambda_j - k^2}\right], & \text{if } z \in (-\infty, -d), \end{cases} \tag{3.8}$$

with A_j defined, up to a sign, by the normalization condition

$$\int_{-\infty}^{0} \phi_j^2(z)dz = \frac{A_j^2}{2}\left[d + \left(\lambda_j^2 - k^2\right)^{-1/2}\right] = 1. \tag{3.9}$$

Note from equation (3.8) that the eigenfunctions decay exponentially for $z < -d$. As explained in section 3.(c), they define the propagating modes $\phi_j(z)\exp\left[\pm i\sqrt{\lambda_j}\,x\right]$ which are trapped near the thin layer, and represent the surface waves in our model.

(b) The eigenfunctions that define the body and evanescent waves

The remaining eigenvalues $(\lambda_j)_{j \geq N_s+1}$ lie in the spectral interval $(-\infty, k^2)$. The eigenfunctions are of the form

$$\phi_j(z) = \begin{cases} A_j \sin\left[z\sqrt{k^2n^2-\lambda_j}\right], & \text{if } z \in (-d, 0), \\ B_j \cos\left[(D+z)\sqrt{k^2-\lambda_j}\right], & \text{if } z \in (-D, -d), \end{cases} \tag{3.10}$$

with constants A_j and B_j related by

$$B_j = -A_j \frac{\sin\left[d\sqrt{k^2n^2-\lambda_j}\right]}{\cos\left[(D-d)\sqrt{k^2-\lambda_j}\right]}, \tag{3.11}$$

so that (3.10) is continuous at $z = -d$. The normalization condition $\int_{-D}^{0} \phi_j^2(z)dz = 1$ defines A_j up to a sign, and as shown in appendix B, in the regime $kD \gg 1$ we have

$$A_j^2 \simeq \frac{2(k^2-\lambda_j)}{D\left[k^2-\lambda_j + k^2(n^2-1)\cos^2\left(d\sqrt{k^2n^2-\lambda_j}\right)\right]}, \qquad B_j^2 \simeq \frac{2}{D}. \tag{3.12}$$

As in the previous section, the continuity of the derivative of (3.10) gives that the eigenvalues satisfy the equation

$$\tan\left[d\sqrt{k^2n^2-\lambda}\right]\tan\left[(D-d)\sqrt{k^2-\lambda}\right] = \frac{\sqrt{k^2n^2-\lambda}}{\sqrt{k^2-\lambda}}. \tag{3.13}$$

Let N_b denote the number of positive eigenvalues $\lambda_j \in (0, k^2)$. We show in the next section that the corresponding eigenfunctions define the propagating modes $\phi_j(z)\exp\left[\pm i\sqrt{\lambda_j}x\right]$ which are large throughout the section of the waveguide, and represent the body waves in our model. The eigenfunctions for the remaining infinitely many eigenvalues[2] lying in the interval $(-\infty, 0)$ define the evanescent modes $\phi_j(z)\exp\left[-\sqrt{|\lambda_j|}|x|\right]$.

[2]There is a unique sequence of values of D for which $\lambda = 0$ is a solution of (3.13). We assume throughout that even as D grows, it does so outside this set of measure zero.

When D grows, the eigenvalue density increases in $(0, k^2)$, and as proved in appendix B, we have the approximate recursive relation

$$\lambda_j - \lambda_{j+1} \simeq \frac{2\pi}{D}\sqrt{k^2-\lambda_j}, \qquad j = N_{\rm s}+1, \dots, N_{\rm s}+N_{\rm b}. \tag{3.14}$$

This leads to the following estimate of the number of body waves

$$N_{\rm b} \approx \frac{D}{2\pi}\sum_{j=N_{\rm s}+1}^{N_{\rm s}+N_{\rm b}} \frac{\lambda_j-\lambda_{j+1}}{\sqrt{k^2-\lambda_j}} \approx \frac{D}{2\pi}\int_0^{k^2}\frac{d\lambda}{\sqrt{k^2-\lambda}} = \frac{kD}{\pi}. \tag{3.15}$$

(c) Mode decomposition in the unperturbed waveguide

We can use the orthonormal $L^2(-D,0)$ basis of eigenfunctions $\big(\phi_j(z)\big)_{j\geq 1}$ to write the solution $p_0(x,z)$ of (2.1)–(2.2), with $n_\varepsilon^2(x,z)$ replaced by $\mathrm{n}_0^2(z)$, as the following series

$$p_0(x,z) = \sum_{j=1}^{\infty} p_{j,0}(x)\phi_j(z). \tag{3.16}$$

Each term in this series is called a waveguide mode, and $p_{j,0}(x)$ are one-dimensional waves, the solutions of

$$(\partial_x^2 + \lambda_j)p_{j,0}(x) = \delta'(x)\int_{-D}^0 f(z)\phi_j(z)dz, \quad j\geq 1, \tag{3.17}$$

that are outgoing and bounded at $|x|\to\infty$. There are two types of such waves, depending on the sign of the eigenvalue λ_j. If $\lambda_j>0$, then $p_{j,0}(x)$ is a propagating wave. Otherwise, it is an evanescent wave.

The expression of the wave field is

$$p_0(x,z) = \begin{cases} \displaystyle\sum_{j=1}^{N}\frac{a_{j,0}}{\sqrt{\beta_j}}e^{i\beta_j x}\phi_j(z) + \sum_{j\geq N+1}\frac{a_{j,0}}{\sqrt{\beta_j}}e^{-\beta_j x}\phi_j(z), & x>0, \\ \displaystyle -\sum_{j=1}^{N}\frac{a_{j,0}}{\sqrt{\beta_j}}e^{-i\beta_j x}\phi_j(z) - \sum_{j\geq N+1}\frac{a_{j,0}}{\sqrt{\beta_j}}e^{\beta_j x}\phi_j(z), & x<0, \end{cases} \tag{3.18}$$

where $N = N_{\rm s}+N_{\rm b}$ is the total number of propagating modes, and we introduced the notation

$$\beta_j = \sqrt{|\lambda_j|}, \qquad j\geq 1. \tag{3.19}$$

As explained in section 3.(a), the first $N_{\rm s}$ propagating modes are essentially supported in the surface layer, so they model surface waves. The remaining $N_{\rm b}$ propagating modes are called body waves, because as shown in section 3.(b), their transverse profile occupies the entire cross-section of the waveguide.

Since the problem in the unperturbed waveguide is separable, the modes are independent, with constant amplitudes determined by the source

$$a_{j,0} = \frac{\sqrt{\beta_j}}{2}\int_{-D}^0 f(z)\phi_j(z)dz, \qquad j\geq 1. \tag{3.20}$$

(d) Mode decomposition in the randomly perturbed waveguide

The solution of (2.1)–(2.2), with the random coefficient $n_\varepsilon^2(x,z)$ defined in (2.3), can also be expanded in the orthonormal eigenbasis

$$p(x,z) = \sum_{j=1}^{\infty} p_j(x)\phi_j(z), \tag{3.21}$$

but the modes are no longer independent due to scattering in the random medium. Instead, the one-dimensional waves $p_j(x)$, for $j\geq 1$, solve the infinite system of coupled ordinary differential

equations

$$(\partial_x^2+\lambda_j)p_j(x)=\delta'(x)\int_{-D}^{0}f(z)\phi_j(z)dz-k^2\varepsilon 1_{(0,L_\varepsilon)}(x)\sum_{l=1}^{\infty}\mu_{jl}(x)p_l(x), \tag{3.22}$$

driven over the range interval $(0,L_\varepsilon)$ by the random, stationary, mean zero processes

$$\mu_{jl}(x)=\int_{-d}^{0}\phi_j(z)\phi_l(z)\nu(x,z)dz, \qquad j,l\geq 1. \tag{3.23}$$

Here $1_{(0,L_\varepsilon)}(x)$ is the indicator function equal to 1 for $x\in(0,L_\varepsilon)$ and 0 otherwise.

The propagating waves $p_j(x)$, indexed by $j=1,\ldots,N$, have both forward and backward going components. At $x<0$ they satisfy the same equation and radiation condition as in the unperturbed medium, so we can write directly their expression

$$p_j(x)=\frac{b_j^-}{\sqrt{\beta_j}}e^{-i\beta_j x}, \qquad x<0, \qquad j=1,\ldots,N, \tag{3.24}$$

with constant b_j^- to be determined. For $x>0$ we use the method of variation of parameters for second-order ordinary differential equations. We introduce the complex-valued amplitudes of the forward and backward going waves $a_j(x)$ and $b_j(x)$ defined by

$$\begin{aligned}a_j(x)=&\frac{1}{2}\Big(\sqrt{\beta_j}p_j(x)+\frac{1}{i\sqrt{\beta_j}}\partial_x p_j(x)\Big)e^{-i\beta_j x},\\ b_j(x)=&\frac{1}{2}\Big(\sqrt{\beta_j}p_j(x)-\frac{1}{i\sqrt{\beta_j}}\partial_x p_j(x)\Big)e^{i\beta_j x}, \quad j=1,\ldots,N.\end{aligned} \tag{3.25}$$

They satisfy the relation

$$\partial_x a_j(x)e^{i\beta_j x}+\partial_x b_j(x)e^{-i\beta_j x}=0, \qquad j=1,\ldots,N, \tag{3.26}$$

so that

$$\begin{aligned}p_j(x)=&\frac{1}{\sqrt{\beta_j}}\Big(a_j(x)e^{i\beta_j x}+b_j(x)e^{-i\beta_j x}\Big),\\ \partial_x p_j(x)=&i\sqrt{\beta_j}\Big(a_j(x)e^{i\beta_j x}-b_j(x)e^{-i\beta_j x}\Big), \quad j=1,\ldots,N.\end{aligned} \tag{3.27}$$

Using the jump conditions at $x=0$, where the source lies,

$$p_j(0^+)-p_j(0^-)=\int_{-D}^{0}f(z)\phi_j(z)dz, \qquad \partial_x p_j(0^+)=\partial_x p_j(0^-), \tag{3.28}$$

we obtain that[3]

$$a_j(0^+)=a_{j,0}=\frac{\sqrt{\beta_j}}{2}\int_{-D}^{0}f(z)\phi_j(z)dz, \qquad b_j^-=b_j(0^+)-a_{j,0}, \tag{3.29}$$

while the radiation condition at $x\to\infty$ gives

$$b_j(x)=0, \qquad x\geq L_\varepsilon, \qquad j=1,\ldots,N. \tag{3.30}$$

The cumulative scattering effect of the random medium on the propagating wave is now modeled by the random amplitudes $a_j(x)$ and $b_j(x)$, for $j=1,\ldots,N$. Their evolution is described by the following system of first-order ordinary differential equations, obtained by substituting

[3]Because we assume a smooth covariance $\mathcal{C}$ of the random fluctuations, we will see in section 4.(a) that the back reflection from the random medium, captured by $b_j(0)$, is negligible when $\varepsilon\to 0$. Therefore, equation (3.24) gives that at $z<0$ the wave is approximately the same as in the unperturbed waveguide.

equation (3.27) into (3.22) and using (3.26)

$$\partial_x a_j(x) = \frac{ik^2\varepsilon}{2}\sum_{l=1}^{N}\frac{\mu_{jl}(x)}{\sqrt{\beta_l\beta_j}}\left[a_l(x)e^{i(\beta_l-\beta_j)x} + b_l(x)e^{-i(\beta_l+\beta_j)x}\right] + \frac{ik^2\varepsilon}{2}\sum_{l\geq N+1}\frac{\mu_{jl}(x)}{\sqrt{\beta_j}}p_l(x)e^{-i\beta_j x}, \tag{3.31}$$

$$\partial_x b_j(x) = -\frac{ik^2\varepsilon}{2}\sum_{l=1}^{N}\frac{\mu_{jl}(x)}{\sqrt{\beta_l\beta_j}}\left[a_l(x)e^{i(\beta_l+\beta_j)x} + b_l(x)e^{-i(\beta_l-\beta_j)x}\right] - \frac{ik^2\varepsilon}{2}\sum_{l\geq N+1}\frac{\mu_{jl}(x)}{\sqrt{\beta_j}}p_l(x)e^{i\beta_j x}, \tag{3.32}$$

for $x \in (0, L_\varepsilon)$, with initial condition (3.29) and end condition (3.30). This system of $2N$ equations is coupled with the second-order equations (3.22) for the evanescent waves $p_l(x)$, indexed by $l \geq N+1$.

4. Effective dynamics for the mode amplitudes

Let us rename the complex mode amplitudes in the large-range scaling as

$$a_j^\varepsilon(x) = a_j\Big(\frac{x}{\varepsilon^2}\Big), \quad b_j^\varepsilon(x) = b_j\Big(\frac{x}{\varepsilon^2}\Big), \quad j = 1, \dots, N. \tag{4.1}$$

We are interested in their behavior in the limit $\varepsilon \to 0$. The stochastic asymptotic analysis is quite involved, but it follows exactly the lines of the analysis in [1,12] and [10, Chapter 20]. Therefore, we do not repeat it here and just give in section 4.(a) a brief summary and the relevant results for this paper. The radiative transfer equation for the propagating mean mode powers is derived from these results in section 4.(b).

(a) The stochastic limit $\varepsilon \to 0$

The first step in carrying out the limit is to express the evanescent waves $\big(p_l(x/\varepsilon^2)\big)_{l\geq N+1}$ in terms of the propagating mode amplitudes, so that we obtain a closed system of $2N$ ordinary differential equations for $\big(a_j^\varepsilon(x), b_j^\varepsilon(x)\big)_{j=1}^N$. This can be done by inverting the operator $\partial_x^2 + \lambda_j$ in (3.22), for $\lambda_j < 0$, using the Green's function $G_j(x,x') = \frac{1}{2\beta_j}e^{-\beta_j|x-x'|}$. This satisfies

$$(\partial_x^2 - \beta_j^2)G_j(x,x') = -\delta(x-x'),$$

and the radiation condition $G_j(x,x') \to 0$ as $|x-x'| \to \infty$. Green's identity transforms (3.22) into an integral equation with ε perturbed term, which can be solved using Neumann series as shown in [1, Section 3.3] and [10, Section 20.2]. The result is

$$p_j\Big(\frac{x}{\varepsilon^2}\Big) = \frac{\varepsilon k^2}{2\beta_j}\int_0^{L/\varepsilon^2} e^{-\beta_j\left|\frac{x}{\varepsilon^2}-x'\right|}\sum_{l=1}^{N}\frac{\mu_{jl}(x')}{\sqrt{\beta_l}}\Big[a_l^\varepsilon(x)e^{i\beta_l x'} + b_l^\varepsilon(x)e^{-i\beta_l x'}\Big]dx' + O(\varepsilon^2),$$

for $x > 0$ and $j \geq N+1$. Substituting into (3.31)–(3.32) we obtain a closed system of equations for the propagating mode amplitudes.

The assumed smoothness in x of the covariance function (2.4) and therefore the fast decay of its $x-$Fourier transform, the power spectral density $\widehat{\mathcal{C}}(\kappa, z, z')$, implies that in the limit $\varepsilon \to 0$ the coupling between the forward-going amplitudes $\big(a_j^\varepsilon(x)\big)_{j=1}^N$ and the backward-going amplitudes $\big(b_j^\varepsilon(x)\big)_{j=1}^N$ is negligible [12, Section 3.3]. Due to the homogeneous end condition (3.30), we then conclude that

$$b_j^\varepsilon(x) \approx 0, \quad j = 1, \dots, N, \quad x > 0.$$

This is the forward-scattering approximation and the problem reduces to solving an initial value problem for the system of N equations for $\big(a_j^\varepsilon(x)\big)_{j=1}^N$, starting from the values (3.29) at $x = 0$. We can finally apply a diffusion-approximation theorem [10, Chapter 6] to this system and obtain the following result.

Theorem 4.1. *As $\varepsilon \to 0$, the $\mathbb{C}^N$-valued random process $(a_j^\varepsilon(x))_{j=1}^N$ converges in distribution in $C^0([0,L],\mathbb{C}^N)$, the space of continuous functions from $[0,L]$ to $\mathbb{C}^N$, to the Markov process $(\mathfrak{a}_j(x))_{j=1}^N$ with infinitesimal generator $\mathcal{L}$. This generator has the form $\mathcal{L} = \mathcal{L}^{(1)} + \mathcal{L}^{(2)}$, where $\mathcal{L}^{(1)}$ and $\mathcal{L}^{(2)}$ are the differential operators:*

$$\begin{aligned}\mathcal{L}^{(1)} =& \frac{1}{2}\sum_{j,l=1}^{N}(1-\delta_{jl})\Gamma_{jl}^c\big(\mathfrak{a}_j\overline{\mathfrak{a}_j}\partial_{\mathfrak{a}_l}\partial_{\overline{\mathfrak{a}_l}} + \mathfrak{a}_l\overline{\mathfrak{a}_l}\partial_{\mathfrak{a}_j}\partial_{\overline{\mathfrak{a}_j}} - \mathfrak{a}_j\mathfrak{a}_l\partial_{\mathfrak{a}_j}\partial_{\mathfrak{a}_l} - \overline{\mathfrak{a}_j\mathfrak{a}_l}\partial_{\overline{\mathfrak{a}_j}}\partial_{\overline{\mathfrak{a}_l}}\big)\\ &+ \frac{1}{2}\sum_{j,l=1}^{N}\Gamma_{jl}^p\big(\mathfrak{a}_j\overline{\mathfrak{a}_l}\partial_{\mathfrak{a}_j}\partial_{\overline{\mathfrak{a}_l}} + \overline{\mathfrak{a}_j}\mathfrak{a}_l\partial_{\overline{\mathfrak{a}_j}}\partial_{\mathfrak{a}_l} - \mathfrak{a}_j\mathfrak{a}_l\partial_{\mathfrak{a}_j}\partial_{\mathfrak{a}_l} - \overline{\mathfrak{a}_j\mathfrak{a}_l}\partial_{\overline{\mathfrak{a}_j}}\partial_{\overline{\mathfrak{a}_l}}\big)\\ &+ \frac{1}{2}\sum_{j=1}^{N}\big(\Gamma_{jj}^c - \Gamma_{jj}^p\big)\big(\mathfrak{a}_j\partial_{\mathfrak{a}_j} + \overline{\mathfrak{a}_j}\partial_{\overline{\mathfrak{a}_j}}\big) + \frac{i}{2}\sum_{j=1}^{N}\Gamma_{jj}^s\big(\mathfrak{a}_j\partial_{\mathfrak{a}_j} - \overline{\mathfrak{a}_j}\partial_{\overline{\mathfrak{a}_j}}\big), \end{aligned} \tag{4.2}$$

$$\mathcal{L}^{(2)} = i\sum_{j=1}^{N}\kappa_j\big(\mathfrak{a}_j\partial_{\mathfrak{a}_j} - \overline{\mathfrak{a}_j}\partial_{\overline{\mathfrak{a}_j}}\big). \tag{4.3}$$

Here we use the classical complex derivative: if $\zeta = \zeta_r + i\zeta_i$, then $\partial_\zeta = (1/2)(\partial_{\zeta_r} - i\partial_{\zeta_i})$ and $\partial_{\overline{\zeta}} = (1/2)(\partial_{\zeta_r} + i\partial_{\zeta_i})$. The coefficients in (4.2-4.3) are defined as follows:
- For all $j,l = 1,\dots,N$, with $j \neq l$, Γ_{jl}^c and Γ_{jl}^s are given by

$$\Gamma_{jl}^c = \frac{k^4}{2\beta_j\beta_l}\int_0^\infty \mathcal{C}_{jl}(x)\cos\big[(\beta_l-\beta_j)x\big]dx, \qquad \Gamma_{jl}^s = \frac{k^4}{2\beta_j\beta_l}\int_0^\infty \mathcal{C}_{jl}(x)\sin\big[(\beta_l-\beta_j)x\big]dx, \tag{4.4}$$

with $\mathcal{C}_{jl}(x)$ defined by

$$\mathcal{C}_{jl}(x) = \mathbb{E}[\mu_{jl}(0)\mu_{jl}(x)], \tag{4.5}$$

where[4]

$$\mathbb{E}[\mu_{jl}(0)\mu_{j'l'}(x)] \overset{(3.23)}{=} \int_{-d}^{0}\int_{-d}^{0}\phi_j(z)\phi_l(z)\mathcal{C}(x,z,z')\phi_{j'}(z')\phi_{l'}(z')dzdz'. \tag{4.6}$$

- For all $j,l = 1,\dots,N$:

$$\Gamma_{jl}^p = \frac{k^4}{4\beta_j\beta_l}\int_0^\infty\Big\{\mathbb{E}\big[\mu_{jj}(0)\mu_{ll}(x)\big] + \mathbb{E}\big[\mu_{ll}(0)\mu_{jj}(x)\big]\Big\}dx. \tag{4.7}$$

- For all $j = 1,\dots,N$:

$$\Gamma_{jj}^c = -\sum_{l=1,l\neq j}^{N}\Gamma_{jl}^c, \qquad \Gamma_{jj}^s = -\sum_{l=1,l\neq j}^{N}\Gamma_{jl}^s, \qquad \kappa_j = \sum_{l=N+1}^{\infty}\frac{k^4}{2\beta_l\beta_j}\int_0^\infty \mathcal{C}_{jl}(x)\cos(\beta_j x)e^{-\beta_l x}dx. \tag{4.8}$$

We remark that the operator $\mathcal{L}^{(1)}$ models the effect of the coupling between the propagating modes, and we show in the next section that it determines the power exchange between these modes. The operator $\mathcal{L}^{(2)}$ is due to the coupling with the evanescent modes and gives rise to additional phase terms (effective dispersion) of the limit amplitudes of the propagating modes. However, it has no effect on the transfer of power among these modes.

[4]Note that the integrals in (4.6) are computed on the domain $z \in (-d, 0)$ where the random medium lies, and not the entire cross-section of the waveguide.

One can verify by direct calculation that

$$\mathcal{L}\Big(\sum_{j=1}^{N}|\mathfrak{a}_j|^2\Big)=0, \tag{4.9}$$

so the process $(\mathfrak{a}_j(x))_{j=1}^N$ is supported on the sphere of $\mathbb{C}^N$ centered at 0 and with radius R, where

$$R^2=\sum_{l=1}^{N}|a_{l,0}|^2. \tag{4.10}$$

The operator $\mathcal{L}$ is not self-adjoint on this sphere, due to the terms Γ^s_{jj} and κ_j, so the process is not reversible. However, the uniform measure on the sphere is invariant and $\mathcal{L}$ is strongly elliptic. This implies that $(\mathfrak{a}_j(x))_{j=1}^N$ is an ergodic process and its distribution converges as $x\to\infty$ to the uniform distribution over the sphere.

Note that Theorem 4.1 uses the forward scattering approximation. If backscattering is significant, then our analysis cannot be readily extended, because we lose the Markov property that is instrumental in the proof of the diffusion-approximation theorem.

(b) The radiative transfer equation

Denote the limit mode powers by

$$\mathfrak{P}_j(x)=|\mathfrak{a}_j(x)|^2,\qquad j=1,\dots,N. \tag{4.11}$$

If the generator $\mathcal{L}$ described in Theorem 4.1 is applied to a test function that depends only on these mode powers, then the result is a function that depends only on the mode powers, as well. This leads to the following corollary:

Corollary 4.1. *The process $(|a_j^\varepsilon(x)|^2)_{j=1}^N$ converges in the limit $\varepsilon\to 0$ to a Markov process $(\mathfrak{P}_j(x))_{j=1}^N$ whose infinitesimal generator $\mathcal{L}_\mathfrak{P}$ is given by*

$$\mathcal{L}_\mathfrak{P}=\sum_{j\neq l}\Gamma^c_{jl}\big[\mathfrak{P}_l\mathfrak{P}_j(\partial_{\mathfrak{P}_j}-\partial_{\mathfrak{P}_l})\partial_{\mathfrak{P}_j}+(\mathfrak{P}_l-\mathfrak{P}_j)\partial_{\mathfrak{P}_j}\big], \tag{4.12}$$

with Γ^c_{jl} defined in (4.4).

It is easy to conclude from the form of the generator (4.12) that the nth-order moments of the mode powers satisfy closed equations. We are particularly interested in the mean mode powers

$$P_j(x)=\mathbb{E}[\mathfrak{P}_j(x)], \tag{4.13}$$

and obtain, using Corollary 4.1, that they satisfy the following system of radiative transfer equations

$$\partial_x P_j(x)=\sum_{l=1}^{N}\Gamma^c_{jl}\big[P_l(x)-P_j(x)\big],\quad x>0,\qquad P_j(0)=|a_{j,0}|^2,\qquad j=1,\dots,N. \tag{4.14}$$

These equations can be solved explicitly using the exponential of the matrix $\boldsymbol{\Gamma}^c=\big(\Gamma^c_{j,l}\big)_{j,l=1}^N$

$$\boldsymbol{P}(x)=\exp\big(\boldsymbol{\Gamma}^c x\big)\boldsymbol{P}(0),\qquad \boldsymbol{P}(x)=\big(P_1(x),\dots,P_N(x)\big)^T. \tag{4.15}$$

We can estimate the initial cumulative (total) power of the propagating modes $\|\boldsymbol{P}(0)\|_1=R^2$ using equations (4.10), (3.20) and (3.19), as follows

$$\|\boldsymbol{P}(0)\|_1=\sum_{j=1}^{N}\frac{\lambda_j}{4}\left|\int_{-D}^{0}f(z)\phi_j(z)dz\right|^2<\frac{n^2k^2}{4}\sum_{j=1}^{N}\left|\int_{-D}^{0}f(z)\phi_j(z)dz\right|^2<\frac{n^2k^2}{4}\|f\|^2_{L^2}. \tag{4.16}$$

Here the first inequality is because $\lambda_j \in (0, n^2k^2)$ for $j = 1, \ldots, N$ and the second inequality is by Parseval's identity for the expansion in the orthonormal eigenbasis $(\phi_j(z))_{j\geq 1}$. Thus, the total power is uniformly bounded with respect to D and therefore $N_{\rm b}$, when f is square integrable.

In the next section we use equation (4.15) to analyze the transfer of power between the surface and the body waves and the transition to equipartition.

5. Convergence to equipartition

Equation (4.15) shows that the evolution of the mean mode powers is dictated by the matrix $\boldsymbol{\Gamma}^c$ with off-diagonal entries (4.4) and diagonal entries (4.8). Note that the off-diagonal entries are non-negative, because they are power spectral densities of stationary random processes, and that the rows sum to 0. Therefore, 0 is an eigenvalue, for the un-normalized eigenvector $\mathbf{1}_N$ with all entries equal to 1.

We assume henceforth that $\boldsymbol{\Gamma}^c$ is an irreducible matrix. This is a very weak assumption and it means that there are not too many zeros in $\boldsymbol{\Gamma}^c$, which is typical for the covariance functions used in our analysis. More precisely, the assumption is that for any pair $j \neq l$, there exists m and a sequence $j_0, \ldots, j_m$ with $j_0 = j$ and $j_m = l$, so that $\Gamma^c_{j_p, j_{p+1}} > 0$ for all $p = 0, \ldots, m-1$. We can then conclude from the Perron-Frobenius theorem that 0 is the largest eigenvalue, which is simple. This implies that the mean mode power vector (4.15) converges to a vector that is a multiple of $\mathbf{1}_N$ as $x \to \infty$. That is to say, the system reaches equipartition, where the power is distributed uniformly over the modes. The range at which equipartition is reached is the reciprocal of the absolute value of the largest non-zero eigenvalue of $\boldsymbol{\Gamma}^c$ [10, Chapter 20].

In this section we study how the surface and body waves interact during the transition to equipartition, by taking a second limit $kD \to \infty$. Recall that the width d of the surface layer is fixed and of the order of the wavelength, so the number $N_{\rm s}$ of surface wave modes converges to the positive and finite limit (3.7). Recall also from equation (3.15) that the number $N_{\rm b} = N - N_{\rm s}$ of body waves is proportional to kD. Therefore, taking $kD \to \infty$ is equivalent to letting $N_{\rm b} \to \infty$.

To carry out the analysis, we sort the entries in $\boldsymbol{\Gamma}^c$ based on how they depend on $N_{\rm b}$. We see from equations (3.8)–(3.9) that the first $N_{\rm s}$ mode profiles have a finite limit as $kD \to \infty$. Therefore, the block $\left(\Gamma^c_{j,l}\right)_{j,l=1}^{N_{\rm s}}$ has $O(1)$ entries. The body wave profiles are supported in $(-D, 0)$ and have amplitudes of order $\sqrt{2/D} = O(\sqrt{k/N_{\rm b}})$, by (3.10)–(3.12). Using these estimates in definition (4.4) we get that $\boldsymbol{\Gamma}^c$ has the following block structure

$$\boldsymbol{\Gamma}^c = \begin{pmatrix} \boldsymbol{\Gamma}^{(0)} - \boldsymbol{\Lambda} & \frac{1}{N_{\rm b}}\boldsymbol{\Gamma}^{(1)} \\ \frac{1}{N_{\rm b}}{\boldsymbol{\Gamma}^{(1)}}^T & \frac{1}{N_{\rm b}^2}\boldsymbol{\Gamma}^{(2)} - \frac{1}{N_{\rm b}}\widetilde{\boldsymbol{\Lambda}} \end{pmatrix} \tag{5.1}$$

where the blocks $\boldsymbol{\Gamma}^{(0)}, \boldsymbol{\Gamma}^{(1)}, \boldsymbol{\Lambda}$ and $\widetilde{\boldsymbol{\Lambda}}$ have $O(1)$ entries, while the block $\boldsymbol{\Gamma}^{(2)}$ has $O(1)$ off-diagonal entries.

The entries in the off-diagonal block $\boldsymbol{\Gamma}^{(1)} \in \mathbb{R}^{N_{\rm s} \times N_{\rm b}}$ are just the scaled version of those in $\boldsymbol{\Gamma}^c$,

$$\Gamma^{(1)}_{jl} = N_{\rm b}\Gamma^c_{j(l+N_{\rm s})}, \qquad j = 1, \ldots, N_{\rm s}, \;\; l = 1, \ldots, N_{\rm b}. \tag{5.2}$$

The first diagonal block in (5.1) is the difference of two $N_{\rm s} \times N_{\rm s}$ matrices: The first one is $\boldsymbol{\Gamma}^{(0)}$ with entries

$$\Gamma^{(0)}_{jl} = \Gamma^c_{jl}, \quad 1 \leq j, l \leq N_{\rm s}, \;\; j \neq l, \qquad \Gamma^{(0)}_{jj} = -\sum_{l=1 \neq j}^{N_{\rm s}} \Gamma^{(0)}_{jl}, \quad 1 \leq j \leq N_{\rm s}, \tag{5.3}$$

whose rows are summing to zero. The second matrix $\boldsymbol{\Lambda}$ is diagonal, with positive entries

$$\Lambda_{jj} = \frac{1}{N_{\rm b}} \sum_{l=1}^{N_{\rm b}} \Gamma^{(1)}_{jl}, \qquad 1 \leq j \leq N_{\rm s}. \tag{5.4}$$

The second diagonal block in (5.1) is the difference of two $N_\mathrm{b} \times N_\mathrm{b}$ matrices: The first one is defined by $\boldsymbol{\Gamma}^{(2)}$ with off-diagonal entries $\Gamma^{(2)}_{jl}$ and rows summing to zero,

$$\Gamma^{(2)}_{jj} = -\sum_{l=1\neq j}^{N_\mathrm{b}} \Gamma^{(2)}_{jl}, \qquad 1 \leq j \leq N_\mathrm{b}, \tag{5.5}$$

and the second one is defined by the diagonal matrix $\widetilde{\boldsymbol{\Lambda}}$ with nonnegative entries

$$\widetilde{\Lambda}_{jj} = \sum_{l=1}^{N_\mathrm{s}} \Gamma^{(1)}_{lj}, \qquad 1 \leq j \leq N_\mathrm{b}. \tag{5.6}$$

Note that both diagonal blocks of $\boldsymbol{\Gamma}^c$ are negative definite, symmetric matrices.

In the next two sections we use this block structure of $\boldsymbol{\Gamma}^c$ to carry out the analysis of convergence to equipartition. We begin in section 5.(a) with a simplified model which allows a quick and explicit convergence analysis that gives some insight into how the surface and body waves interact. Then we consider the general model in section 5.(b) and we discuss the results in section 5.(c).

(a) Simplified model

Consider the particular case where the entries in the blocks $\boldsymbol{\Gamma}^{(1)}$ and $\boldsymbol{\Gamma}^{(2)}$ satisfy

$$\Gamma^{(1)}_{jl} = \gamma_1, \qquad 1 \leq j \leq N_\mathrm{s}, \;\; 1 \leq l \leq N_\mathrm{b}, \tag{5.7}$$

$$\Gamma^{(2)}_{jl} = \gamma_2, \qquad 1 \leq j, l \leq N_\mathrm{b}, \qquad j \neq l, \tag{5.8}$$

for some positive constants γ_1 and γ_2. Then, the diagonal matrices (5.4) and (5.6) are multiples of the identity matrices $\mathbf{I}_{N_\mathrm{s}} \in \mathbb{R}^{N_\mathrm{s}\times N_\mathrm{s}}$ and $\mathbf{I}_{N_\mathrm{b}} \in \mathbb{R}^{N_\mathrm{b}\times N_\mathrm{b}}$:

$$\boldsymbol{\Lambda} = \gamma_1 \mathbf{I}_{N_\mathrm{s}}, \qquad \widetilde{\boldsymbol{\Lambda}} = N_\mathrm{s}\gamma_1 \mathbf{I}_{N_\mathrm{b}}, \tag{5.9}$$

and we can obtain an explicit spectral decomposition of $\boldsymbol{\Gamma}^c$, for any N_b (large or not):

Let us denote by $-g_1, \ldots, -g_{N_\mathrm{s}}$ the eigenvalues of $\boldsymbol{\Gamma}^{(0)}$ sorted in decreasing order. Note that $\boldsymbol{v}_1 = \frac{1}{\sqrt{N_\mathrm{s}}}\mathbf{1}_{N_\mathrm{s}}$ is an eigenvector of $\boldsymbol{\Gamma}^{(0)}$, for the eigenvalue 0, where we recall that $\mathbf{1}_{N_\mathrm{s}}$ is the vector in $\mathbb{R}^{N_\mathrm{s}}$ with all entries equal to 1. In fact, by the Perron-Frobenius theorem, $-g_1 = 0$ is the leading eigenvalue and it is simple. Since $\boldsymbol{\Gamma}^{(0)}$ is symmetric, it can be diagonalized

$$\boldsymbol{\Gamma}^{(0)} = \mathbf{V}\,\mathrm{Diag}\big(0, -g_2, \ldots, -g_{N_\mathrm{s}}\big)\mathbf{V}^T, \tag{5.10}$$

where $\mathbf{V}$ is the orthogonal matrix of the eigenvectors $(\boldsymbol{v}_j)_{j=1}^{N_\mathrm{s}}$. Similarly, we can diagonalize $\boldsymbol{\Gamma}^{(2)}$

$$\boldsymbol{\Gamma}^{(2)} = \gamma_2 \mathbf{1}_{N_\mathrm{b}}\mathbf{1}_{N_\mathrm{b}}^T - \gamma_2 N_\mathrm{b}\mathbf{I}_{N_\mathrm{b}} = \boldsymbol{W}\,\mathrm{Diag}\big(0, -\gamma_2 N_\mathrm{b}, \ldots, -\gamma_2 N_\mathrm{b}\big)\boldsymbol{W}^T, \tag{5.11}$$

where $\boldsymbol{W} = (\boldsymbol{w}_j)_{j=1}^{N_\mathrm{b}}$ is an orthogonal matrix with first column $\boldsymbol{w}_1 = \frac{1}{\sqrt{N_\mathrm{b}}}\mathbf{1}_{N_\mathrm{b}}$.

Using these spectral decompositions and the relations

$$\boldsymbol{\Gamma}^{(1)}\boldsymbol{w}_j = \sqrt{N_\mathrm{s}N_\mathrm{b}}\boldsymbol{v}_1\delta_{j1}, \quad 1 \leq j \leq N_\mathrm{b}, \qquad \boldsymbol{\Gamma}^{(1)^T}\boldsymbol{v}_j = \sqrt{N_\mathrm{s}N_\mathrm{b}}\boldsymbol{w}_1\delta_{j1}, \quad 1 \leq j \leq N_\mathrm{s}, \tag{5.12}$$

we obtain that $\boldsymbol{\Gamma}^c$ has the following eigenvalues (sorted in decreasing order) and orthonormal eigenvectors:

- The first eigenvalue is simple and equal to 0, for the eigenvector $\frac{1}{\sqrt{N}}\mathbf{1}_N$, as expected from the Perron-Frobenius theorem.
- The next eigenvalue is equal to $-(\gamma_2 + \gamma_1 N_\mathrm{s})/N_\mathrm{b}$, and approaches 0 as $N_\mathrm{b} \to \infty$. This eigenvalue has multiplicity $N_\mathrm{b} - 1$ and the corresponding eigenvectors are $\big(\mathbf{0}^T, \boldsymbol{w}_j^T\big)^T$, for $j = 2, \ldots, N_\mathrm{b}$.
- The next eigenvalue is equal to $-\gamma_1\big(1 + N_\mathrm{s}/N_\mathrm{b}\big)$. It is simple, and has the finite limit $-\gamma_1$ as $N_\mathrm{b} \to \infty$. The eigenvector is $\Big(\sqrt{N_\mathrm{b}/N}\boldsymbol{v}_1^T, -\sqrt{N_\mathrm{s}/N}\boldsymbol{w}_1^T\Big)^T$.

- The remaining $N_\mathrm{s}-1$ eigenvalues $-(g_j+\gamma_1)$ are the eigenvalues of $\boldsymbol{\Gamma}^{(0)}$ shifted by $-\gamma_1$. The eigenvectors are $\left(\boldsymbol{v}_j^T,\mathbf{0}^T\right)^T$, for $j=2,\ldots,N_\mathrm{s}$.

Let us organize the surface wave powers in the vector $\boldsymbol{S}(x)=\left(P_1(x),\ldots,P_{N_\mathrm{s}}(x)\right)^T$ and the body wave powers in the vector $\boldsymbol{B}(x)=\left(P_{N_\mathrm{s}+1}(x),\ldots,P_N(x)\right)^T$. With the explicit spectral decomposition of $\boldsymbol{\Gamma}^c$ given above, we can now calculate the matrix exponential in (4.15) and obtain that the mean powers of the surface waves are

$$\boldsymbol{S}(x)=\frac{R_{\mathrm{s},0}^2}{N}\Big\{1+\frac{N_\mathrm{b}}{N_\mathrm{s}}\exp\big[-\gamma_1(1+N_\mathrm{s}/N_\mathrm{b})x\big]\Big\}\mathbf{1}_{N_\mathrm{s}}+\frac{R_{\mathrm{b},0}^2}{N}\Big\{1-\exp\big[-\gamma_1(1+N_\mathrm{s}/N_\mathrm{b})x\big]\Big\}\mathbf{1}_{N_\mathrm{s}}$$
$$+\sum_{j=2}^{N_\mathrm{s}}\exp\big[-(g_j+\gamma_1)x\big]\left(\boldsymbol{v}_j^T\boldsymbol{S}_0\right)\boldsymbol{v}_j, \tag{5.13}$$

and the mean powers of the body waves are

$$\boldsymbol{B}(x)=\frac{R_{\mathrm{s},0}^2}{N}\Big\{1-\exp\big[-\gamma_1(1+N_\mathrm{s}/N_\mathrm{b})x\big]\Big\}\mathbf{1}_{N_\mathrm{b}}+\frac{R_{\mathrm{b},0}^2}{N}\Big\{1+\frac{N_\mathrm{s}}{N_\mathrm{b}}\exp\big[-\gamma_1(1+N_\mathrm{s}/N_\mathrm{b})x\big]\Big\}\mathbf{1}_{N_\mathrm{b}}$$
$$+\exp\Big[-\frac{(\gamma_2+\gamma_1N_\mathrm{s})}{N_\mathrm{b}}x\Big]\Big(\boldsymbol{B}_0-\frac{R_{\mathrm{b},0}^2}{N_\mathrm{b}}\mathbf{1}_{N_\mathrm{b}}\Big). \tag{5.14}$$

Here we let

$$\boldsymbol{S}_0=\boldsymbol{S}(0)=\left(|a_{1,0}|^2,\ldots,|a_{N_\mathrm{s},0}|^2\right)^T \text{ and } \boldsymbol{B}_0=\boldsymbol{B}(0)=\left(|a_{N_\mathrm{s}+1,0}|^2,\ldots,|a_{N,0}|^2\right)^T$$

be the vectors of initial powers, determined by the source excitation, and we introduced the initial cumulative powers of the surface and body waves

$$R_{\mathrm{s},0}^2=\sum_{j=1}^{N_\mathrm{s}}P_j(0),\qquad R_{\mathrm{b},0}^2=\sum_{j=N_\mathrm{s}+1}^{N}P_j(0). \tag{5.15}$$

Observe that summing in equations (5.13)–(5.14) we get

$$\sum_{j=1}^{N}P_j(x)=R_{\mathrm{s},0}^2+R_{\mathrm{b},0}^2=R^2. \tag{5.16}$$

This is the conservation of energy described in section 4.(a) and equations (4.9)–(4.10).

The fastest decay in equation (5.13) is exhibited by the terms in the last sum. For range $x>(g_2+\gamma_1)^{-1}$ this sum becomes negligible and the mean surface wave powers become equipartitioned. However, even though the power is uniformly distributed among these waves, their cumulative power still evolves

$$R_\mathrm{s}^2(x)=\sum_{j=1}^{N_\mathrm{s}}P_j(x)=\frac{R^2N_\mathrm{s}}{N}+\frac{(R_{\mathrm{s},0}^2N_\mathrm{b}-R_{\mathrm{b},0}^2N_\mathrm{s})}{N}\exp\big[-\gamma_1(1+N_\mathrm{s}/N_\mathrm{b})x\big], \tag{5.17}$$

on the length scale $\left[\gamma_1(1+N_\mathrm{s}/N_\mathrm{b})\right]^{-1}\approx\gamma_1^{-1}$. This is due to the slow dynamics of the power exchange with the body waves.

The last term in equation (5.14) shows that the body waves relaxation to equipartition happens on the very large length scale $N_\mathrm{b}/(\gamma_2+N_\mathrm{s}\gamma_1)$. After this distance, the exponentials in the first two terms of (5.14) are essentially zero and the body waves are in equipartition, with net power $R_\mathrm{b}^2(x)=\sum_{j=N_\mathrm{s}+1}^{N}P_j(x)$ equal to R^2N_b/N. The net power of the surface waves tends to the constant R^2N_s/N by (5.17).

In summary, this simple model reveals that while approaching the equipartition regime, the surface and body wave power exchange occurs as follows:

- First, the surface waves undergo a rapid relaxation towards equipartition amongst themselves, on the range scale $(g_2+\gamma_1)^{-1}$.

- Then, there is a slower conversion mechanism between the surface waves and the body waves on the range scale γ_1^{-1}.
- The body waves undergo a very slow relaxation towards equipartition, on the range scale $N_\mathrm{b}/(\gamma_2 + N_\mathrm{s}\gamma_1)$.
- Once the body waves reach equipartition, the whole system is in equipartition.

Note that even if we set $\gamma_2 = 0$, meaning that there is no conversion among the body waves, we still have convergence to equipartition of the body waves by the mechanism "conversion from body waves to surface waves" followed by "conversion from surface waves to body waves". In general, the comparison between γ_2 and $N_\mathrm{s}\gamma_1$ tells us which mechanism is dominant to achieve this equipartition: the first mechanism governs the direct conversion between body waves, while the second one governs the conversion mediated by surface waves. The first mechanism dominates the second one if $\gamma_2 > N_\mathrm{s}\gamma_1$.

Note also that the surface waves reach equipartition among themselves as soon as x is larger than the first range scale $(g_2 + \gamma_1)^{-1}$, while the body waves reach equipartition only when x is larger than the third range scale $N_\mathrm{b}/(\gamma_2 + N_\mathrm{s}\gamma_1)$. As we will see below, the fact that the surface modes reach a metastable equilibrium at the first range scale is a universal feature, but that this metastable equilibrium is a uniform distribution is very special and happens only for the simplified model. In general the metastable equilibrium of the surface modes slowly evolves at the third range scale and eventually becomes uniform when the body waves reach equipartition, as we will see below.

(b) General model

In the general case it is not possible to get an explicit spectral decomposition of the matrix $\boldsymbol{\Gamma}^c$, but we can obtain estimates of the mean mode powers as we now explain. Let us denote by

$$\boldsymbol{\Gamma} = \boldsymbol{\Gamma}^{(0)} - \boldsymbol{\Lambda}, \qquad \widetilde{\boldsymbol{\Gamma}} = \frac{\boldsymbol{\Gamma}^{(2)}}{N_b} - \widetilde{\boldsymbol{\Lambda}}, \tag{5.18}$$

the diagonal blocks in (5.1) and recall that they are symmetric, diagonally dominant and negative definite matrices. The matrix $\boldsymbol{\Gamma}$ has size $N_\mathrm{s} \times N_\mathrm{s}$ and $O(1)$ entries, $\widetilde{\boldsymbol{\Gamma}}$ has size $N_\mathrm{b} \times N_\mathrm{b}$, $O(1)$ diagonal entries, and $O(1/N_\mathrm{b})$ off-diagonal entries. The matrix $\boldsymbol{\Gamma}^{(1)}$ that defines the off-diagonal blocks in (5.1) has size $N_\mathrm{s} \times N_\mathrm{b}$ and $O(1)$ entries.

Integrating the radiative transfer equation (4.14) we obtain that

$$\boldsymbol{S}(x) = \exp(\boldsymbol{\Gamma} x)\boldsymbol{S}_0 + \frac{1}{N_\mathrm{b}}\int_0^x \exp(\boldsymbol{\Gamma} x')\boldsymbol{\Gamma}^{(1)}\boldsymbol{B}(x - x')dx', \tag{5.19}$$

$$\boldsymbol{B}(x) = \exp\left(\widetilde{\boldsymbol{\Gamma}}\frac{x}{N_\mathrm{b}}\right)\boldsymbol{B}_0 + \frac{1}{N_\mathrm{b}}\int_0^x \exp\left(\widetilde{\boldsymbol{\Gamma}}\frac{x'}{N_\mathrm{b}}\right)\boldsymbol{\Gamma}^{(1)^T}\boldsymbol{S}(x - x')dx', \tag{5.20}$$

where we recall from the previous section that $\boldsymbol{S}(x) \in \mathbb{R}^{N_\mathrm{s}}$ and $\boldsymbol{B}(x) \in \mathbb{R}^{N_\mathrm{b}}$ are the vectors of mean powers of the surface and body waves and $\boldsymbol{S}_0 = \boldsymbol{S}(0)$ and $\boldsymbol{B}_0 = \boldsymbol{B}(0)$ are the vectors of initial powers determined by the source. We use next these equations to analyze how scattering redistributes the power at $x > 0$.

(i) Mean powers at intermediate range $x \ll N_\mathrm{b}$

We show in appendix C that for range $0 < x \ll N_\mathrm{b}$, the mean powers of the surface modes are

$$\begin{aligned}\boldsymbol{S}(x) = &\Big\{ \exp\left(\boldsymbol{\Gamma} x\right) + \frac{1}{{N_\mathrm{b}}^2}\int_0^x \exp\left(\boldsymbol{\Gamma}(x - x')\right)\boldsymbol{\Gamma}^{-1}\boldsymbol{\Gamma}^{(1)}\boldsymbol{\Gamma}^{(1)^T}\exp\left(\boldsymbol{\Gamma} x'\right)dx' \\ &- \frac{1}{{N_\mathrm{b}}^2}\boldsymbol{\Gamma}^{-1}\boldsymbol{\Gamma}^{(1)}\boldsymbol{\Gamma}^{(1)^T}\boldsymbol{\Gamma}^{-1}\left[\exp\left(\boldsymbol{\Gamma} x\right) - \mathbf{I}_{N_\mathrm{s}}\right]\Big\}\boldsymbol{S}_0 \\ &+ \frac{1}{N_\mathrm{b}}\boldsymbol{\Gamma}^{-1}\left[\exp\left(\boldsymbol{\Gamma} x\right) - \mathbf{I}_{N_\mathrm{s}}\right]\boldsymbol{\Gamma}^{(1)}\boldsymbol{B}_0 + o\Big(\frac{R^2}{N_\mathrm{b}}\Big).\end{aligned} \tag{5.21}$$

Since $\boldsymbol{\Gamma}^{(1)}$ is an $N_\mathrm{s} \times N_\mathrm{b}$ matrix with $O(1)$ entries, we note that $\boldsymbol{\Gamma}^{(1)}\boldsymbol{\Gamma}^{(1)^T}$ is an $N_\mathrm{s} \times N_\mathrm{s}$ matrix with $O(N_\mathrm{b})$ entries. The vector $\boldsymbol{\Gamma}^{(1)}\boldsymbol{B}_0$ has $O(R_{\mathrm{b},0}^2)$ entries, which are bounded independent of N_b, as follows from (4.16). Therefore, the terms written explicitly in (5.21) are at least $O(R^2/N_\mathrm{b})$, whereas the residual is $o(R^2/N_\mathrm{b})$.

We also obtain in appendix C the following estimate of the mean powers of the body modes at range $1 \ll x \ll N_\mathrm{b}$:

$$\boldsymbol{B}(x) = \exp\left(\widetilde{\boldsymbol{\Gamma}}\frac{x}{N_\mathrm{b}}\right)\boldsymbol{B}_0 + \frac{1}{N_\mathrm{b}}\boldsymbol{\Gamma}^{(1)^T}\boldsymbol{\Gamma}^{-1}\left[\exp\left(\boldsymbol{\Gamma}x\right) - \mathbf{I}_{N_\mathrm{s}}\right]\boldsymbol{S}_0 + o\Big(\frac{R^2}{N_\mathrm{b}}\Big). \tag{5.22}$$

These expressions reveal the multi-scale nature of the evolution of the mode powers: The surface wave powers evolve quickly, on a range scale $O(1)$, after which the exponentials in (5.21) become negligible and we get the approximate expression (see appendix C):

$$\boldsymbol{S}(x) \approx -\frac{1}{N_\mathrm{b}}\boldsymbol{\Gamma}^{-1}\boldsymbol{\Gamma}^{(1)}\boldsymbol{B}_0 + \frac{1}{{N_\mathrm{b}}^2}\boldsymbol{\Gamma}^{-1}\boldsymbol{\Gamma}^{(1)}\boldsymbol{\Gamma}^{(1)^T}\boldsymbol{\Gamma}^{-1}\boldsymbol{S}_0, \quad \text{for } 1 \ll x \ll N_\mathrm{b}, \tag{5.23}$$

where the range x dependence is in the lower-order terms. This result is similar to what we saw in the simplified model, but the distribution of power among the surface waves is not uniform, unless the entries in $\boldsymbol{\Gamma}^{(1)}$ are equal to each other, as assumed in section 5.(a). Also similar to the results in section 5.(a), the body wave powers evolve slowly on a range scale of order N_b. At shorter range they can be approximated by the expression

$$\boldsymbol{B}(x) \approx \exp\left(\widetilde{\boldsymbol{\Gamma}}\frac{x}{N_\mathrm{b}}\right)\boldsymbol{B}_0 - \frac{1}{N_\mathrm{b}}\boldsymbol{\Gamma}^{(1)^T}\boldsymbol{\Gamma}^{-1}\boldsymbol{S}_0, \quad \text{for } 1 \ll x \ll N_\mathrm{b}. \tag{5.24}$$

(ii) Mean powers at range $x = O(N_\mathrm{b})$

It is only at range $x = N_\mathrm{b}X$, with $X = O(1)$, that the power transfer among the body waves becomes significant, as seen from the following expression derived in appendix C

$$\boldsymbol{B}(N_\mathrm{b}X) \approx \exp\left[\left(\widetilde{\boldsymbol{\Gamma}} - \frac{1}{N_\mathrm{b}}\boldsymbol{\Gamma}^{(1)^T}\boldsymbol{\Gamma}^{-1}\boldsymbol{\Gamma}^{(1)}\right)X\right]\left[\boldsymbol{B}_0 - \frac{1}{N_\mathrm{b}}\boldsymbol{\Gamma}^{(1)^T}\boldsymbol{\Gamma}^{-1}\boldsymbol{S}_0\right]. \tag{5.25}$$

Moreover, the body waves interact with the surface waves whose mean powers become

$$\begin{aligned}\boldsymbol{S}(N_\mathrm{b}X) &\approx -\frac{1}{N_\mathrm{b}}\boldsymbol{\Gamma}^{-1}\boldsymbol{\Gamma}^{(1)}\boldsymbol{B}(N_\mathrm{b}X) \qquad (5.26)\\ &\overset{(5.25)}{\approx} -\frac{1}{N_\mathrm{b}}\boldsymbol{\Gamma}^{-1}\boldsymbol{\Gamma}^{(1)}\exp\left[\left(\widetilde{\boldsymbol{\Gamma}} - \frac{1}{N_\mathrm{b}}\boldsymbol{\Gamma}^{(1)^T}\boldsymbol{\Gamma}^{-1}\boldsymbol{\Gamma}^{(1)}\right)X\right]\left[\boldsymbol{B}_0 - \frac{1}{N_\mathrm{b}}\boldsymbol{\Gamma}^{(1)^T}\boldsymbol{\Gamma}^{-1}\boldsymbol{S}_0\right].\end{aligned}$$

(iii) Equipartition

We now use equations (5.25)–(5.26) to show the convergence to equipartition: We prove in appendix D the following identity,

$$\frac{1}{N_\mathrm{b}}\boldsymbol{\Gamma}^{-1}\boldsymbol{\Gamma}^{(1)}\mathbf{1}_{N_\mathrm{b}} = -\mathbf{1}_{N_\mathrm{s}}, \tag{5.27}$$

which in conjunction with (5.26) shows that the surface wave powers are in equipartition, as soon as the body waves $\boldsymbol{B}(N_\mathrm{b}X)$ reach equipartition.

It remains to describe the convergence of the body wave powers to equipartition, which is dictated in (5.25) by the exponential of the matrix

$$\widetilde{\boldsymbol{\Gamma}} - \frac{1}{N_\mathrm{b}}\boldsymbol{\Gamma}^{(1)^T}\boldsymbol{\Gamma}^{-1}\boldsymbol{\Gamma}^{(1)} \overset{(5.18)}{=} \frac{1}{N_\mathrm{b}}\boldsymbol{\Gamma}^{(2)} - \widetilde{\boldsymbol{\Lambda}} - \frac{1}{N_\mathrm{b}}\boldsymbol{\Gamma}^{(1)^T}\boldsymbol{\Gamma}^{-1}\boldsymbol{\Gamma}^{(1)}. \tag{5.28}$$

The first term in the right-hand side is a symmetric, negative semi-definite matrix with null space $\mathrm{span}\{\mathbf{1}_{N_\mathrm{b}}\}$, and the last term is a positive definite matrix, because $\boldsymbol{\Gamma}$ and thus $\boldsymbol{\Gamma}^{-1}$ are negative definite. The matrix in (5.28) is N_b times the Schur complement of the block $\boldsymbol{\Gamma} = \boldsymbol{\Gamma}^{(0)} - \boldsymbol{\Lambda}$ in the matrix $\boldsymbol{\Gamma}^{(c)}$ in (5.1). By our assumption on $\boldsymbol{\Gamma}^c$, the matrix in (5.28) is nonnegative definite and irreducible, so we can conclude from the Perron-Frobenius theorem that it has a simple leading

eigenvalue, with an eigenvector that has positive entries. The remaining eigenvectors have entries with changing signs, due to orthogonality. We can verify using the identity

$$\frac{1}{N_\mathrm{b}}\boldsymbol{\Gamma}^{(1)^T}\boldsymbol{\Gamma}^{-1}\boldsymbol{\Gamma}^{(1)}\mathbf{1}_{N_\mathrm{b}} = -\widetilde{\boldsymbol{\Lambda}}\mathbf{1}_{N_\mathrm{b}}, \tag{5.29}$$

proved in appendix D, that

$$\begin{aligned}\Big[\widetilde{\boldsymbol{\Gamma}} - \frac{1}{N_\mathrm{b}}\boldsymbol{\Gamma}^{(1)^T}\boldsymbol{\Gamma}^{-1}\boldsymbol{\Gamma}^{(1)}\Big]\mathbf{1}_{N_\mathrm{b}} &\overset{(5.28)}{=} \frac{1}{N_\mathrm{b}}\boldsymbol{\Gamma}^{(2)}\mathbf{1}_{N_\mathrm{b}} - \widetilde{\boldsymbol{\Lambda}}\mathbf{1}_{N_\mathrm{b}} - \frac{1}{N_\mathrm{b}}\boldsymbol{\Gamma}^{(1)^T}\boldsymbol{\Gamma}^{-1}\boldsymbol{\Gamma}^{(1)}\mathbf{1}_{N_\mathrm{b}} \\ &\overset{(5.29)}{=} \frac{1}{N_\mathrm{b}}\boldsymbol{\Gamma}^{(2)}\mathbf{1}_{N_\mathrm{b}} - \widetilde{\boldsymbol{\Lambda}}\mathbf{1}_{N_\mathrm{b}} + \widetilde{\boldsymbol{\Lambda}}\mathbf{1}_{N_\mathrm{b}} \overset{(5.5)}{=} \mathbf{0}.\end{aligned} \tag{5.30}$$

This shows that $\frac{1}{\sqrt{N_\mathrm{b}}}\mathbf{1}_{N_\mathrm{b}}$ must be the leading, normalized eigenvector, for the eigenvalue 0. Consequently, we get from (5.25) that

$$\begin{aligned}\boldsymbol{B}(N_\mathrm{b}X) &\overset{X\to\infty}{\longrightarrow} \frac{1}{N_\mathrm{b}}\left[\mathbf{1}_{N_\mathrm{b}}^T\boldsymbol{B}_0 - \frac{1}{N_\mathrm{b}}\mathbf{1}_{N_\mathrm{b}}^T\boldsymbol{\Gamma}^{(1)^T}\boldsymbol{\Gamma}^{-1}\boldsymbol{S}_0\right]\mathbf{1}_{N_\mathrm{b}} \\ &= \frac{1}{N_\mathrm{b}}\left[\boldsymbol{B}_0^T\mathbf{1}_{N_\mathrm{b}} - \frac{1}{N_\mathrm{b}}\boldsymbol{S}_0^T\boldsymbol{\Gamma}^{-1}\boldsymbol{\Gamma}^{(1)}\mathbf{1}_{N_\mathrm{b}}\right]\mathbf{1}_{N_\mathrm{b}} \\ &\overset{(5.27)}{=} \frac{1}{N_\mathrm{b}}\Big(\boldsymbol{B}_0^T\mathbf{1}_{N_\mathrm{b}} + \boldsymbol{S}_0^T\mathbf{1}_{N_\mathrm{s}}\Big)\mathbf{1}_{N_\mathrm{b}} \approx \frac{R^2}{N}\mathbf{1}_{N_\mathrm{b}},\end{aligned} \tag{5.31}$$

where we used that $\boldsymbol{B}_0^T\mathbf{1}_{N_\mathrm{b}} + \boldsymbol{S}_0^T\mathbf{1}_{N_\mathrm{s}} = \sum_{j=1}^{N} P_j(0) = R^2$ and made the approximation $1/N = 1/(N_\mathrm{b}+N_\mathrm{s}) \approx 1/N_\mathrm{b}$.

Equation (5.31) gives the equipartition of the powers of the body waves, and substituting in (5.26) we get the equipartition of the powers of the surface waves

$$\boldsymbol{S}(N_\mathrm{b}X) \overset{X\to\infty}{\longrightarrow} -\frac{1}{N_\mathrm{b}}\boldsymbol{\Gamma}^{-1}\boldsymbol{\Gamma}^{(1)}\frac{R^2}{N}\mathbf{1}_{N_\mathrm{b}} \overset{(D.1)}{=} \frac{R^2}{N}\mathbf{1}_{N_\mathrm{s}}. \tag{5.32}$$

(c) Discussion

The analysis in the previous two sections shows that the mean powers become equidistributed at range $x \gg N_\mathrm{b}$, but the dynamics is multiscale. The powers of the surface waves relax quickly, on a range scale of $O(1)$ and reach a metastable distribution of power that is in general not uniform, and depends on the entries in the off-diagonal block $\boldsymbol{\Gamma}^{(1)}$ in (5.1). Only when the entries in $\boldsymbol{\Gamma}^{(1)}$ are all equal to γ_1 the distribution of power in the metastable state is uniform. This was obtained in section 5.(a) and to reach the same conclusion from the expression (5.23) we note from definition (5.4) that for such $\boldsymbol{\Gamma}^{(1)}$ we have $\boldsymbol{\Lambda} = \gamma_1\mathbf{I}_{N_\mathrm{s}}$. Then, the first term in (5.23) is

$$\begin{aligned}-\frac{1}{N_\mathrm{b}}\boldsymbol{\Gamma}^{-1}\boldsymbol{\Gamma}^{(1)}\boldsymbol{B}_0 &\overset{(5.18)}{=} -\frac{1}{N_\mathrm{b}}\big(\boldsymbol{\Gamma}^{(0)} - \boldsymbol{\Lambda}\big)^{-1}\boldsymbol{\Gamma}^{(1)}\boldsymbol{B}_0 = -\frac{1}{N_\mathrm{b}}\big(\boldsymbol{\Gamma}^{(0)} - \gamma_1\mathbf{I}_{N_\mathrm{s}}\big)^{-1}\gamma_1 R_{\mathrm{b},0}^2\mathbf{1}_{N_\mathrm{s}} \\ &= \frac{R_{\mathrm{b},0}^2}{N_b}\mathbf{1}_{N_\mathrm{s}} \approx \frac{R_{\mathrm{b},0}^2}{N}\mathbf{1}_{N_\mathrm{s}},\end{aligned} \tag{5.33}$$

where we used that $\boldsymbol{\Gamma}^{(0)}\mathbf{1}_{N_\mathrm{s}} = \mathbf{0}$ and therefore $\big(\boldsymbol{\Gamma}^{(0)} - \gamma_1\mathbf{I}_{N_\mathrm{s}}\big)^{-1}\mathbf{1}_{N_\mathrm{s}} = -\frac{1}{\gamma_1}\mathbf{1}_{N_\mathrm{s}}$. The second term in (5.23) is obtained similarly, using the observation that

$$\boldsymbol{\Gamma}^{-1}\boldsymbol{S}_0 = -\frac{R_{\mathrm{s},0}^2}{N_\mathrm{s}\gamma_1}\mathbf{1}_{N_\mathrm{s}} + \sum_{j=2}^{N_\mathrm{s}}(-g_j - \gamma_1)^{-1}\big[\boldsymbol{v}_j^T\boldsymbol{S}_0\big]\boldsymbol{v}_j,$$

where $-g_j$, for $j = 2,\ldots,N_\mathrm{s}$ are the non-zero eigenvalues of $\boldsymbol{\Gamma}^{(0)}$ and $\boldsymbol{v}_j$ are the eigenvectors, which are orthogonal to the leading one $\frac{1}{\sqrt{N_\mathrm{s}}}\mathbf{1}_{N_\mathrm{s}}$. This implies that

$$\boldsymbol{\Gamma}^{(1)^T}\boldsymbol{v}_j = \mathbf{0}, \qquad j = 2,\ldots,N_\mathrm{s},$$

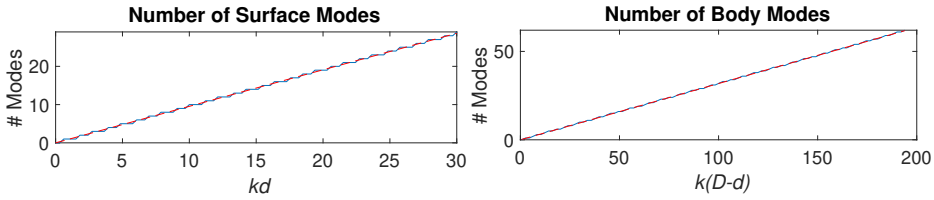

Figure 2. Left: $N_{\rm s}$ vs. kd, for $n^2 = 10$ and $kD = 100$. Right: $N_{\rm b}$ vs. $k(D-d)$ for $n^2 = 10$ and $kd = 6$.

and the second term in (5.23) becomes

$$\frac{1}{{N_{\rm b}}^2}\boldsymbol{\Gamma}^{-1}\boldsymbol{\Gamma}^{(1)}\boldsymbol{\Gamma}^{(1)^T}\boldsymbol{\Gamma}^{-1}\boldsymbol{S}_0 = -\frac{R_{\rm s,0}^2}{{N_{\rm b}}^2 N_{\rm s}\gamma_1}\boldsymbol{\Gamma}^{-1}\boldsymbol{\Gamma}^{(1)}\boldsymbol{\Gamma}^{(1)^T}\mathbf{1}_{N_{\rm s}} = -\frac{R_{\rm s,0}^2}{{N_{\rm b}}^2}\boldsymbol{\Gamma}^{-1}\boldsymbol{\Gamma}^{(1)}\mathbf{1}_{N_{\rm b}}$$
$$= -\frac{R_{\rm s,0}^2\gamma_1}{N_{\rm b}}\boldsymbol{\Gamma}^{-1}\mathbf{1}_{N_{\rm s}} = \frac{R_{\rm s,0}^2}{N_{\rm b}}\mathbf{1}_{N_{\rm s}} \approx \frac{R_{\rm s,0}^2}{N}\mathbf{1}_{N_{\rm s}}. \tag{5.34}$$

We conclude from (5.23), (5.33)–(5.34) and (5.26) that in the special case of $\boldsymbol{\Gamma}^{(1)}$ with all entries equal to γ_1 there is a uniform distribution of the surface wave powers at range $1 \ll x \leq O(N_{\rm b})$, as in section 5.(a).

The body wave powers evolve very slowly, on a range scale $x = O(N_{\rm b})$, and while doing so, they affect the powers of the surface waves. At range $x \gg N_{\rm b}$ the body wave powers become uniformly distributed and this drives the whole system, including the surface waves, to equipartition.

We end the section with the remark that the order of the two limits in our analysis is important. We first let $\varepsilon \to 0$ to derive the radiative transfer equation and then let $kD \to \infty$ i.e., $N_{\rm b} \to \infty$ to analyze the convergence to equipartition. If we took the limit $kD \to \infty$ first, then the domain would be the half space $(x, z) \in \mathbb{R} \times (-\infty, 0)$, with radiation conditions at $z \to -\infty$. The spectrum of the unperturbed Helmholtz operator in the half space has a discrete part, with the $N_{\rm s}$ eigenvalues in the interval (k^2, n^2k^2) defined by equation (3.6), and the corresponding eigenvectors given by (3.8-3.9) that define the surface waves. However, the body waves are replaced by radiation modes, corresponding to the continuous spectrum in $(0, k^2)$. One can establish [11] a convergence result for the discrete mean surface wave powers that reads

$$\partial_x P_j(x) = \sum_{l=1}^{N_{\rm s}} \Gamma_{jl}^{(0)} P_l(x) - \Lambda_{jj} P_j(x), \tag{5.35}$$

with $\boldsymbol{\Gamma}^{(0)}$ given by (5.3) and positive definite, diagonal $\boldsymbol{\Lambda}$. We observe from these equations that $\partial_x \sum_{j=1}^{N_{\rm s}} P_j(x) = -\sum_{j=1}^{N_{\rm s}} \Lambda_{jj} P_j(x) < 0$, so the power carried by the discrete surface modes leaks to the radiating (body) modes. However, there is no feedback from the radiating modes towards the surface modes in this framework, because the range scale required to get this feedback is beyond that of validity of the convergence result for this system. Such feedback is captured in our setting by the radiative transfer equation (4.14), which conserves the total mean power.

6. Numerical illustrations

We now complement the analysis in section 5, carried out in the limit $kD \to \infty$, with numerical simulations for large kD and therefore, large $N_{\rm b}$.

In Fig. 2 we verify the estimates (3.7) and (3.15) of $N_{\rm s}$ and $N_{\rm b}$. We display with the blue lines the numbers of the numerically calculated eigenvalues and with the red lines the estimates $kd\sqrt{n^2-1}/\pi$ (left plot) and $k(D-d)/\pi$ (right plot) for $N_{\rm s}$ and $N_{\rm b}$, respectively.

In Fig. 3 we give the eigenvalues λ_j for $j = 1, \ldots, N_{\rm s}$ in the left plots and $j = N_{\rm s}+1, \ldots, N$ in the right plots. These eigenvalues are calculated by solving equations (3.5) and (3.13). In the left

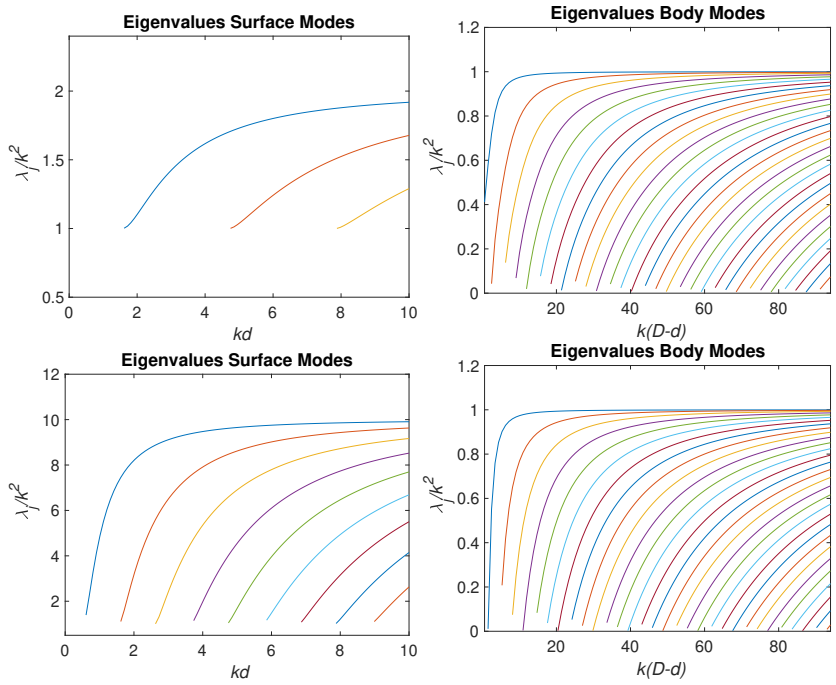

Figure 3. Left column: Eigenvalues in the spectral interval (k^2, n^2k^2). Right column: eigenvalues in the spectral interval $(0, k^2)$. The top plots are for $n^2 = 2$ and the bottom plots are for $n^2 = 10$.

plots we fix $kD = 100$ and vary kd in the interval $(0, 10)$, for two values of the squared index of refraction: $n^2 = 2$ in the top plots and $n^2 = 10$ in the bottom plots. As expected from the estimate (3.7), the number N_s of surface waves grows with kd and with n^2. The right plots show that the number of body waves increases with kD but it is basically independent of n^2, as expected from the results in section 3.(b).

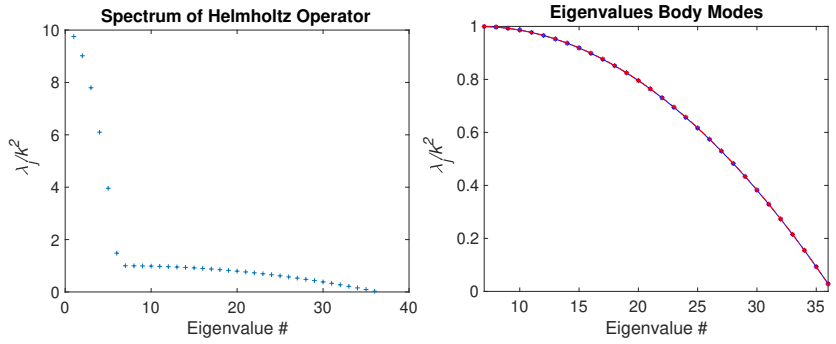

Figure 4. Left: spectrum of the Helmholtz operator for $n^2 = 10$, $kd = 6$ and $kD = 100$. There are 6 eigenvalues in the spectral interval (k^2, n^2k^2), corresponding to the surface waves. The remaining 30 eigenvalues in the interval $(0, k^2)$ are compared in the right plot with the asymptotic expression (6.1) discussed in section 3.(b).

The remaining figures are for $n^2 = 10$, $kd = 6$ and $kD = 100$, so that the spectrum of the Helmholtz operator $\partial_z^2 + k^2 n_0^2(z)$ is as displayed in Fig. 4. There are $N_s = 6$ surface waves and $N_b = 30$ body waves. The right plot in Fig. 4 compares the calculated eigenvalues $(\lambda_j)_{j=7}^{36}$ with

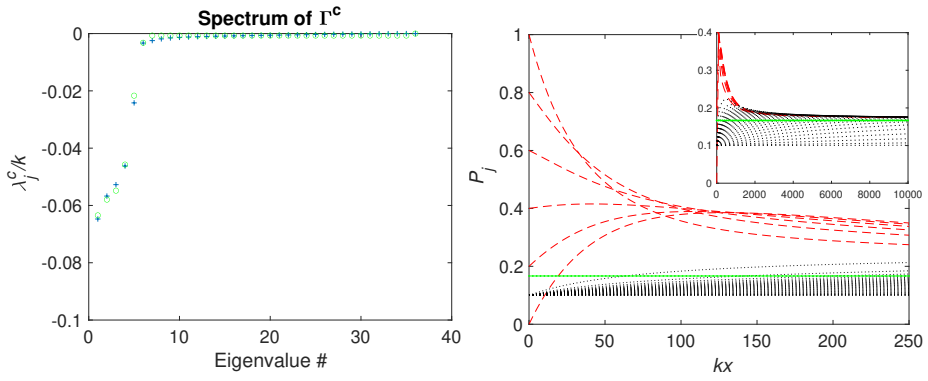

Figure 5. Results for the Gaussian covariance with $\ell = 1/k$. Left: The eigenvalues of $\boldsymbol{\Gamma}^c$ are shown with blue crosses and the estimates $\lambda_j = \theta_{N+1-j}$ with θ_j given by (6.3) are shown with the green circles. Right: Evolution of the mode powers with increasing range x. The surface mode powers are shown with red dashed lines, the body mode powers are shown with black dotted lines, and the green line is the average mode power. The inset corresponds to longer propagation distances (kx up to 10^4) and displays the evolution toward equipartition, albeit very slowly for the body modes.

the approximation (see section 3.(b))

$$\frac{\lambda_j}{k^2} \approx 1 - \frac{(j - N_{\rm s} - 1/2)^2\pi^2}{(D-d)^2}, \qquad N_{\rm s} = 6, \;\; j = 7, \ldots, 36. \tag{6.1}$$

To illustrate the evolution towards equipartition, we consider a Gaussian covariance function (2.4) of the fluctuations of the index of refraction in the surface layer

$$\mathcal{C}(x, z, z') = \exp\Big(- \frac{x^2}{2\ell^2} - \frac{(z-z')^2}{2\ell^2}\Big), \tag{6.2}$$

where ℓ is the correlation length. The entries of $\boldsymbol{\Gamma}^c$ calculated using definitions (4.4) and (4.8) are

$$\Gamma^c_{jl} = \frac{\sqrt{\pi} k^4 \ell}{2\sqrt{2}\beta_j\beta_l} \exp\Big(- \frac{(\beta_l - \beta_j)^2\ell^2}{2}\Big) \int_{-d}^0 \int_{-d}^0 \phi_j(z)\phi_l(z) \exp\Big(- \frac{(z-z')^2}{2\ell^2}\Big)\phi_j(z')\phi_l(z') dz dz',$$

and they have a non-monotone dependence with respect to the correlation length ℓ. Note that the entries Γ^c_{jl} are large when ℓ is somewhat larger than $1/k$, so that the factor $\ell \exp(-(\beta_j - \beta_l)^2\ell^2/2)$ is large, also that the entries tend to zero when ℓ goes to zero or infinity. In the left plot of Fig. 5 we show with blue crosses the eigenvalues of $\boldsymbol{\Gamma}^c$ and with green circles the eigenvalues given in section 5.(a) for the simplified model (5.7)–(5.8). If we denote these eigenvalues by θ_j, for $j = 1, \ldots, N$, and sort the eigenvalues of the simplified model in decreasing order, they are

$$\theta_j = \begin{cases} 0, & \text{if } j = 1, \\ -(\gamma_2 + \gamma_1 N_s)/N_{\rm b}, & \text{if } j = 2, \ldots, N_{\rm b}, \\ -\gamma_1(1 + N_{\rm s}/N_{\rm b}) & \text{if } j = N_{\rm b} + 1, \\ -(g_j + \gamma_1) & \text{if } j = N_{\rm b} + 2, \ldots, N, \end{cases} \tag{6.3}$$

where $-g_j$ are the eigenvalues of $\boldsymbol{\Gamma}^{(0)}$ and the constants γ_1, γ_2 are taken to be the averaged values of the entries of the block matrices:

$$\gamma_1 = \frac{1}{N_{\rm s}} \sum_{j=1}^{N_{\rm s}} \sum_{l=1}^{N_{\rm b}} \Gamma^c_{jl}, \qquad \gamma_2 = \frac{2N_{\rm b}}{(N_{\rm b} - 1)} \sum_{j,l=N_{\rm s}+1}^{N} \Gamma^c_{jl}.$$

Note that even though the entries in the blocks $\boldsymbol{\Gamma}^{(1)}$ and $\boldsymbol{\Gamma}^{(2)}$ of $\boldsymbol{\Gamma}^c$ have O(1) relative variations, the model in section 5.(a) gives good estimates of the eigenvalues.

In the right plot of Fig. 5 we display the evolution of the mode powers with range. The surface mode powers are shown with red lines and the body wave powers with black lines. The average mode power or equipartition limit R^2/N is shown with the green line. As predicted by the theory, we see a rapid relaxation of the surface wave powers that lasts up to the scaled range $kx \approx 50$, after which there is a slow transition towards equipartition. The body mode powers evolve very slowly, as predicted by the analysis.

7. Summary

We introduced a mathematical model for studying the transfer of power between surface and body waves as they transition towards the equilibrium state of equipartition of power. The model is a two-dimensional acoustic waveguide in the domain $(x, z) \in \mathbb{R} \times (-D, 0)$. The waveguide has reflecting boundaries at $z = 0$ and $z = -D$, and a thin "surface" layer of width $d \ll D$, adjacent to the top boundary. This layer is filled with a weakly inhomogeneous random medium, whereas the remainder of the waveguide is filled with a homogeneous medium. There are two kinds of wave modes in the waveguide: those that propagate and those that decay i.e., are evanescent. The propagating modes can be classified further as those that are trapped in the surface layer, and thus model surface waves, and those that penetrate in the entire cross-section of the waveguide and model body waves.

We use asymptotic stochastic analysis to study from first principles the coupling between the propagating and the evanescent modes induced by scattering in the surface layer, and derive a radiative transfer equation for the mean powers of the propagating modes. With this equation we study the evolution of the mode powers in the asymptotic regime $kD \to \infty$. This corresponds to having a finite number of surface waves and an infinite number of body waves. We prove the convergence of the mean mode powers to the equilibrium state of equipartition and show that the dynamics during this convergence is multiscale: The surface wave powers evolve quickly, and reach a metastable state that changes slowly due to the back and forth transfer of power with the body waves. The body wave powers evolve very slowly and eventually reach equipartition. When this happens, the whole system, including the surface waves, is in the equipartition state i.e., the power is distributed uniformly over the modes.

The model presented in this paper seeks to mimic seismic wave propagation in the Earth's crust, which is much more complex due to the presence of different types of surface waves such as Rayleigh and Love waves. It is a first step towards the full understanding of radiative transfer in seismology. The next step should be to incorporate polarization effects for elastic waves (this was done in open media in [24]). Another important point would be to take into account energy absorption, which is expected to affect surface waves because of the presence of fluids in the sub-surface of the Earth.

A. Proof of the statements in section 3.(a)

We begin with the proof that the number of solutions of equation (3.6) in the spectral interval (k^2, k^2n^2) is N_s defined by (3.7).

Proof. λ is a solution in (k^2, n^2k^2) of (3.6) if and only if $t = d\sqrt{k^2n^2 - \lambda}$ is a solution in $(0, kd\sqrt{n^2 - 1})$ of $\psi(t) = \tan(t)$, where the function

$$\psi(t) = -t/\sqrt{k^2d^2(n^2 - 1) - t^2} \tag{A.1}$$

is monotone decreasing from $(0, kd\sqrt{n^2 - 1})$ onto $(-\infty, 0)$, with $\lim_{t \nearrow kd\sqrt{n^2-1}} \psi(t) = -\infty$, as shown in Figure 6. We look for the solutions $t \in (0, kd\sqrt{n^2 - 1})$ of $\psi(t) = \tan(t)$:

- There is no solution in $(0, \pi/2)$ because $\tan(t) > 0$ and $\psi(t) < 0$. There is exactly one solution in $(\pi/2, \pi)$ iff $kd\sqrt{n^2 - 1} > \pi/2$, otherwise there is no solution.
- For any positive integer p: There is no solution in $(p\pi, (p + 1/2)\pi)$ because $\tan(t) > 0$ and $\psi(t) < 0$ and there is exactly one solution in $((p + 1/2)\pi, (p + 1)\pi)$ iff $kd\sqrt{n^2 - 1} > (p + 1/2)\pi$.

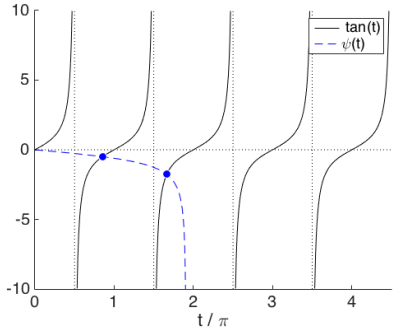

Figure 6. Determination of the solutions of the equation $\psi(t) = \tan(t)$ with $kd\sqrt{n^2-1} = 6$. Here there are $N_s = 2$ solutions (the blue dots).

Otherwise there is no solution. Consequently, the number N_s of solutions is the unique integer such that $(N_s - 1/2)\pi < kd\sqrt{n^2-1} \le (N_s + 1/2)\pi$. This completes the proof of (3.7). □

Now let us describe the eigenfunctions that define the surface waves, which are defined in equations (3.3)–(3.4) for a finite D,

$$\phi_j(z) = \begin{cases} A_j \sin\left[\sqrt{k^2n^2-\lambda_j}\, z\right], & \text{if } z \in (-d, 0), \\ -A_j \sin\left[\sqrt{k^2n^2-\lambda_j}\, d\right] \dfrac{\cosh\left[\sqrt{\lambda_j-k^2}\,(D+z)\right]}{\cosh\left[\sqrt{\lambda_j-k^2}\,(D-d)\right]}, & \text{if } z \in (-D, -d). \end{cases} \tag{A.2}$$

Rewriting the ratio of the cosh functions we obtain that

$$\begin{aligned} \frac{\cosh\left[\sqrt{\lambda_j-k^2}\,(D+z)\right]}{\cosh\left[\sqrt{\lambda_j-k^2}\,(D-d)\right]} &= \frac{\exp\left[\sqrt{\lambda_j-k^2}\,(z+d)\right] + \exp\left[-\sqrt{\lambda_j-k^2}\,(2D+z-d)\right]}{1+\exp\left[-\sqrt{\lambda_j-k^2}\,(2D-2d)\right]} \\ &\approx \exp\left[\sqrt{\lambda_j-k^2}\,(z+d)\right], \end{aligned}$$

where the approximation is for $kD \gg 1$. The expression (3.8) of the eigenfunctions follows in the limit $kD \to \infty$.

It remains to compute the normalizing constant A_j. Direct integration gives

$$\begin{aligned} 1 = \int_{-\infty}^{0} \phi_j^2(z)dz &= \frac{A_j^2}{2}\left[d - \frac{\sin\left[d\sqrt{k^2n^2-\lambda_j}\right]\cos\left[d\sqrt{k^2n^2-\lambda_j}\right]}{\sqrt{k^2n^2-\lambda_j}} + \frac{\sin^2\left[d\sqrt{k^2n^2-\lambda_j}\right]}{\sqrt{\lambda_j-k^2}}\right] \\ &\overset{(3.6)}{=} \frac{A_j^2}{2}\left[d + \frac{\cos^2\left[d\sqrt{k^2n^2-\lambda_j}\right]}{\sqrt{\lambda_j-k^2}} + \frac{\sin^2\left[d\sqrt{k^2n^2-\lambda_j}\right]}{\sqrt{\lambda_j-k^2}}\right] = \frac{A_j^2}{2}\left[d + \frac{1}{\sqrt{\lambda_j-k^2}}\right], \end{aligned}$$

as stated in equation (3.9).

B. Proof of the statements in section 3.(b)

To estimate the number of body waves in the regime $kD \gg 1$, note that in equation (3.13) only $\tan\left[(D-d)\sqrt{k^2-\lambda}\right]$ varies rapidly in λ. The remaining factors are approximately constant over a period of this tangent.

Let λ_j and λ_{j+1} be two consecutive solutions of (3.13), and define

$$\bar{\lambda} := \frac{\lambda_j + \lambda_{j+1}}{2}, \qquad \widetilde{\lambda} := \lambda_j - \lambda_{j+1} > 0. \tag{B.1}$$

Using the observation above, we conclude that

$$D\sqrt{k^2-\lambda_{j+1}}-D\sqrt{k^2-\lambda_j}=D\sqrt{k^2-\bar{\lambda}+\frac{\widetilde{\lambda}}{2}}-D\sqrt{k^2-\bar{\lambda}-\frac{\widetilde{\lambda}}{2}}\approx\pi. \tag{B.2}$$

Squaring this equation and rearranging terms: $\sqrt{(k^2-\bar{\lambda})^2-\widetilde{\lambda}^2/4}\approx k^2-\bar{\lambda}-\pi^2/(2D^2)$. Squaring one more time and solving for $\widetilde{\lambda}$,

$$\widetilde{\lambda}\approx\frac{2\pi}{D}\sqrt{k^2-\bar{\lambda}}\left[1+\frac{\pi^2}{4D^2(k^2-\bar{\lambda})}\right]\approx\frac{2\pi}{D}\sqrt{k^2-\bar{\lambda}}. \tag{B.3}$$

This shows that the separation between the eigenvalues is approximately inverse proportional to D, and in combination with (B.1) it leads to the recursion relation

$$\lambda_j-\lambda_{j+1}\approx\frac{2\pi}{D}\sqrt{k^2-\lambda_j}, \tag{B.4}$$

stated in section 3.(b).

We estimate the normalizing constant A_j of $\phi_j(z)$ using (3.10)

$$\begin{aligned}1=\int_{-D}^{0}\phi_j^2(z)dz=A_j^2\Bigg\{&\frac{(D-d)}{2}\frac{\sin^2\left[d\sqrt{k^2n^2-\lambda_j}\right]}{\cos^2\left[(D-d)\sqrt{k^2-\lambda_j}\right]}+\frac{d}{2}-\frac{1}{4}\sin\left[2d\sqrt{k^2n^2-\lambda_j}\right]\\&\times\left[\frac{\tan\left[d\sqrt{k^2n^2-\lambda_j}\right]\tan\left[(D-d)\sqrt{k^2-\lambda_j}\right]}{\sqrt{k^2-\lambda_j}}-\frac{1}{\sqrt{k^2n^2-\lambda_j}}\right]\Bigg\}\\\overset{(3.13)}{=}A_j^2&\left[\frac{(D-d)}{2}\frac{\sin^2\left[d\sqrt{k^2n^2-\lambda_j}\right]}{\cos^2\left[(D-d)\sqrt{k^2-\lambda_j}\right]}+\frac{d}{2}-\frac{\sin\left[2d\sqrt{k^2n^2-\lambda_j}\right]k^2(n^2-1)}{4(k^2-\lambda_j)\sqrt{k^2n^2-\lambda_j}}\right]\\\approx&\frac{A_j^2D\sin^2\left[d\sqrt{k^2n^2-\lambda_j}\right]}{2\cos^2\left[(D-d)\sqrt{k^2-\lambda_j}\right]}.\end{aligned}$$

This gives that

$$A_j^2\approx\frac{2\cos^2\left[(D-d)\sqrt{k^2-\lambda_j}\right]}{D\sin^2\left[d\sqrt{k^2n^2-\lambda_j}\right]}, \tag{B.5}$$

and therefore, by (3.11), $B_j^2\approx 2/D$. Finally, we rewrite further equation (B.5) using equation (3.13):

$$\begin{aligned}A_j^2\approx\frac{2\cos^2\left[(D-d)\sqrt{k^2-\lambda_j}\right]}{D\sin^2\left[d\sqrt{k^2n^2-\lambda_j}\right]}&=\frac{2}{D\sin^2\left[d\sqrt{k^2n^2-\lambda_j}\right]\left[1+\tan^2\left[(D-d)\sqrt{k^2-\lambda_j}\right]\right]}\\\overset{(3.13)}{=}&\frac{2}{D\left[\sin^2\left[d\sqrt{k^2n^2-\lambda_j}\right]+\frac{(k^2n^2-\lambda_j)}{(k^2-\lambda_j)}\cos^2\left[d\sqrt{k^2n^2-\lambda_j}\right]\right]}\\=&\frac{2(k^2-\lambda_j)}{D\left[k^2-\lambda_j+k^2(n^2-1)\cos^2\left[d\sqrt{k^2n^2-\lambda_j}\right]\right]},\end{aligned} \tag{B.6}$$

as stated in section 3.(b).

C. Estimation of the mean mode powers

Let us begin with the observation that the negative definite diagonal blocks $\boldsymbol{\Gamma}$ and $\widetilde{\boldsymbol{\Gamma}}$ satisfy

$$\exp\left(\boldsymbol{\Gamma}x\right) \approx 0, \quad \text{for } x \gg 1, \tag{C.1}$$

$$\exp\left(\widetilde{\boldsymbol{\Gamma}}\frac{x}{N_\mathrm{b}}\right) = \mathbf{I}_{N_\mathrm{b}} + O\Big(\frac{x}{N_b}\Big), \quad \text{for } 0 < x \ll N_\mathrm{b}, \tag{C.2}$$

$$\exp\left(\widetilde{\boldsymbol{\Gamma}}\frac{x}{N_\mathrm{b}}\right) \to 0, \quad \text{for } \frac{x}{N_b} \to \infty. \tag{C.3}$$

In the next two sections we use these results to estimate the mean mode powers in two distinct range intervals: $x \ll N_\mathrm{b}$ and $x = O(N_\mathrm{b})$.

(a) Estimates at range $x \ll N_\mathrm{b}$

Let us iterate once equations (5.19)–(5.20) and use a change of variable of integration, to obtain

$$\begin{aligned}\boldsymbol{S}(x) = \exp\left(\boldsymbol{\Gamma}x\right)\boldsymbol{S}_0 + \frac{1}{N_\mathrm{b}}\int_0^x \exp\left(\boldsymbol{\Gamma}x'\right)\boldsymbol{\Gamma}^{(1)} \exp\left(\widetilde{\boldsymbol{\Gamma}}\frac{x-x'}{N_\mathrm{b}}\right)\boldsymbol{B}_0 dx' \\ + \frac{1}{{N_\mathrm{b}}^2}\int_0^x \Big[\int_{x'}^x \exp\left(\boldsymbol{\Gamma}(x-x'')\right)\boldsymbol{\Gamma}^{(1)} \exp\left(\widetilde{\boldsymbol{\Gamma}}\frac{x''-x'}{N_\mathrm{b}}\right)dx''\Big]{\boldsymbol{\Gamma}^{(1)}}^T \boldsymbol{S}(x')dx',\end{aligned} \tag{C.4}$$

$$\begin{aligned}\boldsymbol{B}(x) = \exp\left(\widetilde{\boldsymbol{\Gamma}}\frac{x}{N_\mathrm{b}}\right)\boldsymbol{B}_0 + \frac{1}{N_\mathrm{b}}\int_0^x \exp\left(\widetilde{\boldsymbol{\Gamma}}\frac{x'}{N_\mathrm{b}}\right){\boldsymbol{\Gamma}^{(1)}}^T \exp\left(\boldsymbol{\Gamma}(x-x')\right)\boldsymbol{S}_0 dx' \\ + \frac{1}{{N_\mathrm{b}}^2}\int_0^x \Big[\int_{x'}^x \exp\left(\widetilde{\boldsymbol{\Gamma}}\frac{(x-x'')}{N_\mathrm{b}}\right){\boldsymbol{\Gamma}^{(1)}}^T \exp\Big(\boldsymbol{\Gamma}(x''-x')\Big)dx''\Big]\boldsymbol{\Gamma}^{(1)}\boldsymbol{B}(x')dx'.\end{aligned} \tag{C.5}$$

We now use these equations to approximate the vectors $\boldsymbol{S}(x)$ and $\boldsymbol{B}(x)$ of the mean mode powers, as we increase the range x.

We begin with the estimation of $\boldsymbol{S}(x)$: For $x \ll N_\mathrm{b}$, we can replace $\exp\left(\widetilde{\boldsymbol{\Gamma}}\frac{x}{N_\mathrm{b}}\right)$ by $\mathbf{I}_{N_\mathrm{b}}$ and equation (C.4) gives

$$\begin{aligned}\boldsymbol{S}(x) = \exp\left(\boldsymbol{\Gamma}x\right)\boldsymbol{S}_0 + \frac{1}{N_\mathrm{b}}\Big[\int_0^x \exp\left(\boldsymbol{\Gamma}x'\right)dx'\Big]\boldsymbol{\Gamma}^{(1)}\boldsymbol{B}_0 \\ + \frac{1}{{N_\mathrm{b}}^2}\int_0^x \Big[\int_{x'}^x \exp\left(\boldsymbol{\Gamma}(x-x'')\right)dx''\Big]\boldsymbol{\Gamma}^{(1)}{\boldsymbol{\Gamma}^{(1)}}^T\boldsymbol{S}(x')dx' + o\Big(\frac{R^2}{N_\mathrm{b}}\Big),\end{aligned} \tag{C.6}$$

and integrating the exponentials of $\boldsymbol{\Gamma}$ we get

$$\begin{aligned}\boldsymbol{S}(x) = \exp\left(\boldsymbol{\Gamma}x\right)\boldsymbol{S}_0 + \frac{1}{N_\mathrm{b}}\boldsymbol{\Gamma}^{-1}\Big[\exp\left(\boldsymbol{\Gamma}x\right) - \mathbf{I}_{N_\mathrm{s}}\Big]\boldsymbol{\Gamma}^{(1)}\boldsymbol{B}_0 \\ + \frac{1}{{N_\mathrm{b}}^2}\boldsymbol{\Gamma}^{-1}\int_0^x \Big[\exp\left(\boldsymbol{\Gamma}(x-x')\right) - \mathbf{I}_{N_\mathrm{s}}\Big]\boldsymbol{\Gamma}^{(1)}{\boldsymbol{\Gamma}^{(1)}}^T\boldsymbol{S}(x')dx' + o\Big(\frac{R^2}{N_\mathrm{b}}\Big).\end{aligned} \tag{C.7}$$

Note that since $\boldsymbol{\Gamma}^{(1)}$ is an $N_\mathrm{s} \times N_\mathrm{b}$ matrix with $O(1)$ entries, $\boldsymbol{\Gamma}^{(1)}{\boldsymbol{\Gamma}^{(1)}}^T$ is an $N_\mathrm{s} \times N_\mathrm{s}$ matrix with $O(N_\mathrm{b})$ entries. Moreover, the vector $\boldsymbol{\Gamma}^{(1)}\boldsymbol{B}_0 \in \mathbb{R}^{N_\mathrm{s}}$ has $O(R_{\mathrm{b},0}^2)$ entries by (4.16). Thus, the first term in the right-hand side of (C.7) is $O(R^2)$ and the last two terms are of order $O(R^2/N_\mathrm{b})$. Iterating equation (C.7) one time, and using that $\boldsymbol{\Gamma}^{-1}$ commutes with the exponential of $\boldsymbol{\Gamma}$, we obtain equation (5.21).

When we let $1 \ll x \ll N_\mathrm{b}$ in (5.21), and recall that $\boldsymbol{\Gamma}$ is negative definite, we observe that $\exp(\boldsymbol{\Gamma}x)$ goes to zero and the leading-order term involving $\boldsymbol{S}_0$ is $\frac{1}{{N_\mathrm{b}}^2}\boldsymbol{\Gamma}^{-1}\boldsymbol{\Gamma}^{(1)}{\boldsymbol{\Gamma}^{(1)}}^T\boldsymbol{\Gamma}^{-1}\boldsymbol{S}_0$. The leading-order term involving $\boldsymbol{B}_0$ is $-\frac{1}{N_\mathrm{b}}\boldsymbol{\Gamma}^{-1}\boldsymbol{\Gamma}^{(1)}\boldsymbol{B}_0$. We then get from (5.21) that

$$\boldsymbol{S}(x) = -\frac{1}{N_\mathrm{b}}\boldsymbol{\Gamma}^{-1}\boldsymbol{\Gamma}^{(1)}\boldsymbol{B}_0 + \frac{1}{{N_\mathrm{b}}^2}\boldsymbol{\Gamma}^{-1}\boldsymbol{\Gamma}^{(1)}{\boldsymbol{\Gamma}^{(1)}}^T\boldsymbol{\Gamma}^{-1}\boldsymbol{S}_0 + o\Big(\frac{R^2}{N_\mathrm{b}}\Big), \quad \text{for } 1 \ll x \ll N_\mathrm{b}, \tag{C.8}$$

where the first term is $O(R^2)$, the second term is $O(R^2/N_\mathrm{b})$ and the residual tends to zero faster than R^2/N_b in the limit $N_\mathrm{b}\to\infty$.

For the vector of mean mode powers of the body waves at range $x \ll N_\mathrm{b}$ we can approximate the second and third exponentials of $\widetilde{\boldsymbol{\Gamma}}$ in (C.5) by the identity $\mathbf{I}_{N_\mathrm{b}}$ and obtain

$$\boldsymbol{B}(x) = \exp\left(\widetilde{\boldsymbol{\Gamma}}\frac{x}{N_\mathrm{b}}\right)\boldsymbol{B}_0 + \frac{1}{N_\mathrm{b}}\boldsymbol{\Gamma}^{(1)^T}\boldsymbol{\Gamma}^{-1}\left[\exp\left(\boldsymbol{\Gamma}x\right) - \mathbf{I}_{N_\mathrm{s}}\right]\boldsymbol{S}_0 + o\Big(\frac{R^2}{N_\mathrm{b}}\Big), \tag{C.9}$$

which is equation (5.22). The first term in the right-hand side is $O(R^2)$ and the second term is $O(R^2/N_\mathrm{b})$. Finally, at $1 \ll x \ll N_\mathrm{b}$ the approximation becomes

$$\boldsymbol{B}(x) = \exp\left(\widetilde{\boldsymbol{\Gamma}}\frac{x}{N_\mathrm{b}}\right)\boldsymbol{B}_0 - \frac{1}{N_\mathrm{b}}\boldsymbol{\Gamma}^{(1)^T}\boldsymbol{\Gamma}^{-1}\boldsymbol{S}_0 + o\Big(\frac{R^2}{N_\mathrm{b}}\Big). \tag{C.10}$$

(b) Estimates at range $x = O(N_\mathrm{b})$

Let us set $x = N_\mathrm{b}X$, with $X = O(1)$, and use (C.1) in (5.19) to obtain

$$\boldsymbol{S}(N_\mathrm{b}X) \approx \frac{1}{N_\mathrm{b}}\int_0^{N_\mathrm{b}X}\exp(\boldsymbol{\Gamma}x')\boldsymbol{\Gamma}^{(1)}\boldsymbol{B}(N_\mathrm{b}X - x')dx'. \tag{C.11}$$

Due to the decaying exponential, only ranges $x' = O(1)$ contribute to the integral, and we can use the expansion $\boldsymbol{B}(N_\mathrm{b}X - x') \approx \boldsymbol{B}(N_\mathrm{b}X) + O(R^2/N_\mathrm{b})$, where the remainder is because, by (5.20), $\partial_x\boldsymbol{B}(x) = O(R^2/N_\mathrm{b})$. Therefore, we get the expression

$$\begin{aligned}\boldsymbol{S}(N_\mathrm{b}X) &\approx \frac{1}{N_\mathrm{b}}\int_0^{N_\mathrm{b}X}\exp(\boldsymbol{\Gamma}x')dx'\boldsymbol{\Gamma}^{(1)}\boldsymbol{B}(N_\mathrm{b}X)\\ &= \frac{1}{N_\mathrm{b}}\boldsymbol{\Gamma}^{-1}\left[\exp(\boldsymbol{\Gamma}N_\mathrm{b}X) - \mathbf{I}_{N_\mathrm{s}}\right]\boldsymbol{\Gamma}^{(1)}\boldsymbol{B}(N_\mathrm{b}X) \approx -\frac{1}{N_\mathrm{b}}\boldsymbol{\Gamma}^{-1}\boldsymbol{\Gamma}^{(1)}\boldsymbol{B}(N_\mathrm{b}X).\end{aligned} \tag{C.12}$$

The body wave powers satisfy the ordinary differential equation

$$\partial_X\boldsymbol{B}(N_\mathrm{b}X) = \widetilde{\boldsymbol{\Gamma}}\boldsymbol{B}(N_\mathrm{b}X) + \boldsymbol{\Gamma}^{(1)^T}\boldsymbol{S}(N_\mathrm{b}X) \overset{(C.12)}{\approx} \left[\widetilde{\boldsymbol{\Gamma}} - \frac{1}{N_\mathrm{b}}\boldsymbol{\Gamma}^{(1)^T}\boldsymbol{\Gamma}^{-1}\boldsymbol{\Gamma}^{(1)}\right]\boldsymbol{B}(N_\mathrm{b}X). \tag{C.13}$$

Then with the initial condition deriving from (C.10) with $0 < X \ll 1$, we find

$$\boldsymbol{B}(N_\mathrm{b}X) \approx \exp\left[\left(\widetilde{\boldsymbol{\Gamma}} - \frac{1}{N_\mathrm{b}}\boldsymbol{\Gamma}^{(1)^T}\boldsymbol{\Gamma}^{-1}\boldsymbol{\Gamma}^{(1)}\right)X\right]\left[\boldsymbol{B}_0 - \frac{1}{N_\mathrm{b}}\boldsymbol{\Gamma}^{(1)^T}\boldsymbol{\Gamma}^{-1}\boldsymbol{S}_0\right],$$

and substituting into (C.12) we get that

$$\boldsymbol{S}(N_\mathrm{b}X) \approx -\frac{1}{N_\mathrm{b}}\boldsymbol{\Gamma}^{-1}\boldsymbol{\Gamma}^{(1)}\exp\left[\left(\widetilde{\boldsymbol{\Gamma}} - \frac{1}{N_\mathrm{b}}\boldsymbol{\Gamma}^{(1)^T}\boldsymbol{\Gamma}^{-1}\boldsymbol{\Gamma}^{(1)}\right)X\right]\left[\boldsymbol{B}_0 - \frac{1}{N_\mathrm{b}}\boldsymbol{\Gamma}^{(1)^T}\boldsymbol{\Gamma}^{-1}\boldsymbol{S}_0\right].$$

D. Identities needed in the convergence analysis

To derive identity (5.27), let us obtain from definition (5.4) of the diagonal matrix $\boldsymbol{\Lambda}$ that

$$\frac{1}{N_\mathrm{b}}\boldsymbol{\Gamma}^{(1)}\mathbf{1}_{N_\mathrm{b}} = \boldsymbol{\Lambda}\mathbf{1}_{N_\mathrm{s}}. \tag{D.1}$$

This gives $\frac{1}{N_\mathrm{b}}\boldsymbol{\Gamma}^{-1}\boldsymbol{\Gamma}^{(1)}\mathbf{1}_{N_\mathrm{b}} = \boldsymbol{\Gamma}^{-1}\boldsymbol{\Lambda}\mathbf{1}_{N_\mathrm{s}}$, and using that $\boldsymbol{\Lambda} \overset{(5.18)}{=} \boldsymbol{\Gamma}^{(0)} - \boldsymbol{\Gamma}$, we get

$$\frac{1}{N_\mathrm{b}}\boldsymbol{\Gamma}^{-1}\boldsymbol{\Gamma}^{(1)}\mathbf{1}_{N_\mathrm{b}} = \boldsymbol{\Gamma}^{-1}\boldsymbol{\Gamma}^{(0)}\mathbf{1}_{N_\mathrm{s}} - \boldsymbol{\Gamma}^{-1}\boldsymbol{\Gamma}\mathbf{1}_{N_\mathrm{s}} = -\mathbf{1}_{N_\mathrm{s}}, \tag{D.2}$$

where the last equation is because the rows of $\boldsymbol{\Gamma}^{(0)}$ sum to 0. This proves (5.27).

Identity (5.29) follows from this result and the definition (5.6) of $\widetilde{\boldsymbol{\Lambda}}$,

$$\frac{1}{N_\mathrm{b}}\boldsymbol{\Gamma}^{(1)^T}\boldsymbol{\Gamma}^{-1}\boldsymbol{\Gamma}^{(1)}\mathbf{1}_{N_\mathrm{b}} \overset{(D.2)}{=} -\boldsymbol{\Gamma}^{(1)^T}\mathbf{1}_{N_\mathrm{s}} \overset{(5.6)}{=} -\widetilde{\boldsymbol{\Lambda}}\mathbf{1}_{N_\mathrm{b}}. \tag{D.3}$$

Data Accessibility. This article has no additional data. The results are reproducible from the contents of the paper.

Authors' Contributions. L.B., J.G. and K.S. have formulated the problem, carried out the analysis and the statement of results, wrote the paper and contributed to the critical revision. All authors gave final approval for publication and agree to be held accountable for the work performed therein.

Competing Interests. We declare we have no competing interests.

Funding. This research is supported in part by AFOSR grants FA9550-18-1-0131 and FA9550-18-1-0217, by ONR grant N00014-17-1-2057 and NSF grant DMS-2010046. The work of the second author was also supported by the French ANR under Grant No. ANR-19-CE46-0007 (project ICCI).

References

1. R. Alonso, L. Borcea, and J. Garnier, Wave propagation in waveguides with rough boundaries, Commun. Math. Sci. **11**, 233-267 (2012).
2. L. A. Apresyan and Y. A. Kravtsov, Radiation Transfer: Statistical and Wave Aspects, Gordon and Breach, Amsterdam, 1995.
3. S. R. Arridge and J. C. Schotland, Optical tomography: forward and inverse problems, Inverse Problems **25**, 123010 (2009).
4. G. Bal, T. Komorowski, and L. Ryzhik, Kinetic limits for waves in a random medium, Kinetic & Related Models **3**, 529 (2010).
5. L. Borcea and J. Garnier, Polarization effects for electromagnetic wave propagation in random media. Wave Motion **63**, 179-208 (2016).
6. L. Borcea and J. Garnier, Derivation of a one-way radiative transfer equation in random media, Phys. Rev. E **93**, 022115, (2016).
7. M. Campillo and A. Paul, Long-range correlations in the diffuse seismic coda, Science **299**(5606), 547-549 (2003).
8. G. J. Chaplain, J. M. De Ponti, A. Colombi, R. Fuentes-Dominguez, P. Dryburg, D. Pieris, R. J. Smith, A. Clare, M. Clark, and R. V. Craster, Tailored elastic surface to body wave Umklapp conversion, Nature Communications **11**, 1-6, (2020).
9. S. Chandrasekar, Radiative Transfer, Dover Publications, New York, 1960.
10. J.-P. Fouque, J. Garnier, G. Papanicolaou, and K. Sølna, Wave Propagation and Time Reversal in Randomly Layered Media, Springer, New York, 2007.
11. J. Garnier, Intensity fluctuations in random waveguides, Commun. Math. Sci. **18**, 947-971 (2020).
12. J. Garnier and G. Papanicolaou, Pulse propagation and time reversal in random waveguides, SIAM J. Appl. Math. **67**, 1718-1739 (2007).
13. J. Garnier, and K. Sølna, Coupled paraxial wave equations in random media in the white-noise regime, The Annals of Applied Probability **19**, 318-346 (2009).
14. J. Garnier, and K. Sølna, Background velocity estimation by cross correlations of ambient noise signals in radiative transport regime, Comm. Math. Sci. **9**, 743-766 (2011).
15. R. Hennino, N. Trégourès, N. M. Shapiro, L. Margerin, M. Campillo, B. van Tiggelen, and R. L. Weaver, Observation of equipartition of seismic waves, Phys. Rev. Lett. **86**, 3447-3450 (2001).
16. A. Ishimaru, Wave Propagation and Scattering in Random Media, Academic Press, 1978.
17. O. I. Lobkis and R. L. Weaver, On the emergence of the Green's function in the correlations of a diffuse field, J. Acoust. Soc. Am. **110**, 3011-3017 (2001).
18. T. Maeda, H. Sato, and T. Nishimura, Synthesis of coda wave envelopes in randomly inhomogeneous elastic media in a half-space: single scattering model including Rayleigh waves, Geophys. J. Int. **172**, 130-154 (2008).
19. A. E. Malcolm, J. A. Scales and B. A. van Tiggelen, Extracting the Green function from diffuse, equipartitioned waves, Phys. Rev. E **70**, p.015601, (2004).
20. L. Margerin, Introduction to Radiative Transfer of Seismic Waves, in Seismic Earth: Array Analysis of Broadband Seismograms, edited by A. Levander and G. Nolet, Volume 157, Geophysical Monograph Series, American Geophysical Union, Washington, 2005.
21. L. Margerin, A. Bajaras, and M. Campillo, A scalar radiative transfer model including the coupling between surface and body waves, Geophys. J. Int. **219**, 1092-1108 (2019).
22. A. Obermann, T. T. Planès, C. Hadziioannou, and M. Campillo, Lapse-time-dependent coda-wave depth sensitivity to local velocity perturbations in 3-D heterogeneous elastic media, Geophys. J. Int. **207**, 59-66 (2016).

23. G. Poupinet, W.L. Ellsworth, and J. Frechet, Monitoring velocity variations in the crust using earthquake doublets: An application to the Calaveras Fault, California, Journal of Geophysical Research: Solid Earth **89**(B7), 5719-5731 (1984).
24. L. Ryzhik, G. Papanicolaou, and J. B. Keller, Transport equations for elastic and other waves in random media, Wave Motion **24**, 327-370 (1996).
25. H. Sato, M. C. Fehler, and T. Maeda, Seismic Wave Propagation and Scattering in the Heterogeneous Earth, Springer, Berlin, 2012.
26. C. Sens-Schönfelder and E. Larose, Temporal changes in the lunar soil from correlation of diffuse vibrations, Phys. Rev. E **78**, 045601 (2008).
27. C. Sens-Schönfelder and U. Wegler, Passive image interferometry and seasonal variations of seismic velocities at Merapi Volcano, Indonesia, Geophysical Research Letters **33**, L21302 (2006).
28. S. R. Seshadri, Leaky Rayleigh waves, Journal of Applied Physics **73**, 3637-3650, (1993).
29. R. Snieder, Scattering of surface waves, Chapter 1.7.3, pages 562-577, in Scattering and Inverse Scattering in Pure and Applied Sciences, Eds. R. Pike, P. Sabatier, Academic Press, 2002.
30. R. Snieder, A. Grêt, H. Douma, and J. Scales, Coda wave interferometry for estimating nonlinear behavior in seismic velocity, Science **295**(5563), 2253-2255, (2002).
31. N. P. Trégourès and B. A. van Tiggelen, Quasi-two-dimensional transfer of elastic waves, Phys. Rev. E **66**, 036601 (2002).
32. S. Vanlanduit, P. Guillaume, and G. Van Der Linden On-line monitoring of fatigue cracks using ultrasonic surface waves, NDT & E International **36**, 601-607 (2003).
33. R. L. Weaver, On diffuse waves in solid media, J. Acoust. Soc. Am. **71**, 1608-1609 (1982).
34. R. S. Wu, Multiple scattering and energy transfer of seismic waves - separation of scattering effect from intrinsic attenuation I, Theoretical Modelling **82**, 57-80 (1985).
35. Y. Zeng, Scattered surface wave energy in the seismic coda, Pure and Applied Geophysics **163**, 533-548 (2006).